Carolina Maia Vettorazzo

MODEL PREDICTIVE CONTROL OF GAS COMPRESSION STATION IN OFF-SHORE PRODUCTION PLATFORMS

Dissertation presented to the Graduate Program in Automation and Systems Engineering in partial fulfillment of the requirements for the degree of Master in Automation and Systems Engineering.

Advisor: Prof. Agustinho Plucenio, Ph.D
Co-advisor: Prof. Julio Elias Normey-Rico, Ph.D

Florianópolis

2016

Ficha de identificação da obra elaborada pelo autor,
através do Programa de Geração Automática da Biblioteca Universitária da UFSC.

Vettorazzo, Carolina Maia
Model predictive control of gas compression station in off-shore production platforms / Carolina Maia Vettorazzo ; orientador, Agustinho Plucenio; coorientador, Júlio Elias Normey-Rico - SC, 2016.
112 p.

Dissertação (mestrado) - Universidade Federal de Santa Catarina, Centro Tecnológico, Programa de Pós Graduação em Engenharia de Automação e Sistemas, Florianópolis, 2016.

Inclui referências.

1. Engenharia de Automação e Sistemas. 2. Sistemas de compressão. 3. MPC. 4. Ajuste de controladores. I. Plucenio, Agustinho. II. Normey Rico, Júlio Elias. III. Universidade Federal de Santa Catarina. Programa de Pós-Graduação em Engenharia de Automação e Sistemas. IV. Título.

Carolina Maia Vettorazzo

MODEL PREDICTIVE CONTROL OF GAS COMPRESSION STATION IN OFF-SHORE PRODUCTION PLATFORMS

This Dissertation is recommended in partial fulfillment of the requirements for the degree of "Master in Automation and Systems Engineering", which has been approved in its present form by the Graduate Program in Automation and Systems Engineering.

Florianópolis, December 14th 2016.

Prof. Dr. Daniel Ferreira Coutinho
Graduate Program Coordinator
Federal University of Santa Catarina

Dissertation Committee:

Prof. Agustinho Plucenio, Ph.D
Advisor
Federal University of Santa Catarina

Daniel Martins Lima, Ph.D
Federal University of Santa Catarina

Eduardo Camponogara, Ph.D
Federal University of Santa Catarina

Eugênio de Bona Castelan Neto, Ph.D
Federal University of Santa Catarina

À minha família.

ACKNOWLEDGEMENTS

I would like to thank my advisors Prof. Agustinho Plucenio and Prof. Julio Normay-Rico for teaching me. They gave me the opportunity to work with them and inspired me to become a better researcher.

I thank my family and friends for all the support. They believed in my potential even when I did not and kept me on my path during the worst moments. I am very grateful to my partner Marco who was always by my side, even when we were in different time zones.

I thank my research colleagues for all the theoretical discussions and ideas, specially Rafael Sartori and Thaise Damo for the support outside the lab.

I also thank the engineers Marcelo Lima and Mario Campos from Cenpes – Petrobras for their enlightenment on the compressor' theory and ideas.

Finally, I thank the Federal University of Santa Catarina and the Department of Automation and Systems for accepting me in the graduate program, allowing me to use their facilities and resources, and Petrobras funding my research.

"We but mirror the world. All the tendencies present in the outer world are to be found in the world of our body. If we could change ourselves, the tendencies in the world would also change. As a man changes his own nature, so does the attitude of the world change towards him. This is the divine mystery supreme. A wonderful thing it is and the source of our happiness. We need not wait to see what others do."
(Original quote for the saying: "Be the change you wish to see in the world")

– Mahatma Gandhi

RESUMO ESTENDIDO

Uma plataforma *off-shore* normalmente produz petróleo bruto e gás natural. O gás é tratado para a remoção da humidade e sua pressão e sua temperatura são modificadas de acordo com sua aplicação final. Parte do gás é direcionado para a linha de exportação de gás para ser comercializado. Muitas vezes o gás é utilizado por poços que operam com elevação por *gaslift*. O gás natural também é usado em turbinas para gerar eletricidade. Um sistema de compressão de gás é uma parte importante de uma unidade de produção *off-shore* de petróleo. O tipo de compressor mais usado em um sistema de compressão de gás é o compressor centrífugo. Uma falha do compressor pode fazer com que uma unidade de produção completa seja desligada. Os compressores centrífugos têm limites operacionais muito restritos e são muito sensíveis a mudanças na vazão de entrada de gás ou nas propriedades do mesmo. O compressor pode entrar em *surge*, que é uma condição operacional instável caracterizada pelo fluxo reverso de gás dentro do compressor e que pode acontecer quando a vazão de entrada de gás é muito baixa. Um compressor centrífugo que opera em *surge* não comprimirá o gás corretamente, causando danos permanentes à máquina. O procedimento normal utilizado quando se detecta a ocorrência de *surge* é parar o compressor. Geralmente, os compressores centrífugos são instalados com um controle regulatório que inclui a prevenção de *surge*. No entanto, mudanças bruscas na vazão de entrada de gás e na composição do gás são conhecidas por fazer com que o compressor centrífugo pare com freqüência. Esta dissertação propõe um controlador MPC que reduz o consumo de energia do sistema de compressão e melhora sua proteção contra *surge*. Este trabalho também apresenta a modelagem de uma estação de compressão real composta de dois compressores de três estágios. Com base na análise do comportamento do sistema e da relação dinâmica entre as entradas e saídas do sistema, são propostas e testadas duas formulações de MPC diferentes. Para ajustar o controlador MPC foi aplicada a técnica de ajuste satisfatório, melhorando o desempenho do controlador.

Palavras-chave: Sistemas de compressão. MPC. Ajuste de controladores

ABSTRACT

An offshore oil production unit normally produces crude oil and natural gas. The gas is treated for removal of moisture and its pressure and temperature are conditioned to its target application. Part of the gas is directed to the gas export line for sales. Often it is used by wells operating with gas lift. Natural gas is also used in turbines to generate electricity. A gas compression system is an important part of an offshore oil production unit. The most important type of equipment used in a gas compression system is the centrifugal compressor. A compressor failure may cause a complete production unit shut down. Centrifugal compressors have a limited operational range and are very sensitive to changes in the gas flow rate or in its properties. Compressor surge is an unstable operational condition characterized by reverse flow inside the compressor and it can happen when the gas flow rate is too low. A centrifugal compressor operating in surge mode will not compress the gas as required and the machine could be damaged permanently. The normal procedure used when surge is detected is to stop the compressor. Usually centrifugal compressors are installed with a regulatory control that includes the avoidance of surge. But abrupt changes in gas flow-rate and gas composition are known to cause centrifugal compressor to stop the production operations too often. This dissertation proposes a MPC controller that reduces the energy consumption of the compression system and improves its protection against surge. This work also presents the modeling of a real compression station composed of two three-stage compressors. Based on the analysis of the system's behavior and the dynamic relation between inputs and outputs, two different MPC formulations are proposed and tested. To tune the MPC controller the satisficing tuning technique is applied, improving the controller's performance.

Keywords: Compression system. MPC. Tuning.

LIST OF FIGURES

LIST OF TABLES

ACRONYMS

ARIMA	Auto-Regressive Integrated Moving Average
DMC	Dynamic Matrix Control
EHAC	Extended Horizon Adaptive Control
EPSAC	Extended Prediction Self-adaptive Control
GPC	Generalized Predictive Control
MIMO	Multiple Inputs Multiple Outputs
MPC	Model Predictive Control
MTBF	Mean Time Between Failure
SISO	Single Input Single Output

SYMBOLS

A_1	Area of the impeller (m^2)
CV_N	Flow coefficient
G	Dynamic matrix of the system
IS	Index of surge
J	Compressor moment of inertia (kgm^2)
Ki_{exp}	Integral gain of the outlet pressure controller
Kp_{exp}	Proportional gain of the outlet pressure controller
L_c	Length of the duct (m)
MW	Molecular weight of the gas mixture $(kg/kmol)$
Q_{cp}	Gas volume flow rate through the compressor (m^3/s)
Q_{surge}	Minimum gas volume flow rate through the compressor to avoid surge (m^3/s)
Q	Gas volume flow rate (m^3/s)
R	Gas constant (J/mol)
T_d	Discharge temperature of a compression stage (K)
T_s	Suction temperature of a compression stage (K)
V_p	Plenum volume (m^3)
V_h	Outlet header volume, it represents the total volume associated with the pipes (m^3)
V_{in}	Volume of the compressor inlet drum (m^3)
Z	Gas compressibility
$\Psi(\omega, m)$	Compressor characteristic curve
η_p	Polytropic efficiency of the compression
μ	Compressor slip factor
ω	Compressor speed (rad/s)
τ_c	Torque exerted by the compressor load (Nm)
τ_d	Driver torque (Nm)
a_0	Sonic velocity (m/s)
k	Gas specific heat ratio
m_t	Gas mass flow rate through the throttle (kg/s)
m_{exp}	Gas mass flow rate delivered the exportation line (kg/s)
m_{flare}	Gas mass flow rate in the flare line (kg/s)
$m_{in,1}$	Gas mass flow rate entering the compression train 1 (kg/s)
$m_{in,2}$	Gas mass flow rate entering the compression train 2 (kg/s)
m_{in}	Inlet gas mass flow rate (kg/s)
$m_{out,1}$	Gas mass flow rate from compressor train 1 (kg/s)
$m_{out,2}$	Gas mass flow rate from compressor train 2 (kg/s)

m_{out}	Outlet gas mass flow rate (kg/s)
m_{p1}	Gas mass flow rate delivered to process 1 (kg/s)
m_{p2}	Gas mass flow rate delivered to process 2 (kg/s)
m_r	Gas mass flow rate through antisurge valve (kg/s)
m	Gas mass flow rate through the compressor (kg/s)
p_d	Discharge pressure of the compressor stage (bar)
p_p	Pressure in the plenum (Pa)
p_s	Suction pressure of a compression stage (m^3/s)
p_{in}	Pressure in the inlet header (bar)
p_{out}	Pressure in the outlet header (bar)
$p_{s,1}$	Suction pressure of stage 1 of compression train 1 (bar)
$p_{s,2}$	Suction pressure of stage 1 of compression train 2 (bar)
pd_{ij}	Discharge pressure of stage ij, where i refers to the compressor line and j to the compressor stage (bar)
r_2	Impeller radius (m)

CONTENTS

1 INTRODUCTION

The gas compression system is an important component of offshore oil and gas production plants. It is responsible for increasing the pressure of the gas coming from the separator, supplying a certain gas flow rate at specific pressure, humidity, and temperature, according to the desired operating point and the specifications of the subsequent systems. The compressed gas can then be exported, used for gas-lift, used to generate electrical energy, or return to the reservoir in injection wells.

The compression system has to process the gas flow rate delivered by the separator. Stopping a compressor may cause this gas to accumulate and the pressure on the separator to rise above safety limits. In that case the uncompressed gas has to be flared, which is an operation subject to environmental regulation. In critical situations oil wells may have to be closed until the compression system starts to work again.

Oil and gas production facilities are equipped with centrifugal compressors, which have limited operational ranges. A good review of centrifugal compressor applications as well as ways to enhance the capability of the compressor can be found in [3].

One of the main causes of compressor shutdown is the occurrence of a phenomena called surge [4],[5]. Surge is an unstable operation condition of a compressor. It is characterized by alternation of flow directions inside the compressor with oscillations in the gas pressures and flow-rates. Surge usually occurs when the inlet gas flow rate is below specified limits and the pressure ratio is too high [3],[4]. The surge region is one of the operation limitations of centrifugal compressors. Another operation limitation is the stonewall region, which is characterized by high flow-rates with gas velocities around the sound speed. Operation in the stonewall region is normally avoided because of mechanical wear on the compressor. Besides, the compressor manufacturer may recommend maximum and minimum rotation speeds of the shaft.

Given these operation limits the gas flow rate through the compressor can be changed in two ways: the surplus gas can be flared to decrease the gas flow rate or the compressed gas can be recycled back the compressor suction to increase the gas flow rate through the compressor. The gas flaring is handled by the flare valve that opens when the pressure is too high. The recirculation of the compressed gas is handled by the antisurge regulatory control system. It is designed to manipulate the recycle valves in order to keep the compressor operating in a safe region. But changes in the gas

molecular weight with abrupt variations in the gas flow-rate, for example, may cause the regulatory control system to fail and the compressor to go into surge, causing the system to stop. It is known that plant shut-down due to failure in the compression system caused by surge is a recurrent problem.

Usually the solution to the surge problem is to avoid its occurrence [4]. In [6] it is stated that active surge control solutions have been proposed but they are not yet available for industrial applications.

To understand and prevent this phenomena several models have been proposed in the literature. The phenomenological modeling of centrifugal compressors was first presented in 1976 by Greitzer in [7]. He introduces a single stage centrifugal compressor described by a set of differential and algebraic equations. In [8], [2], [5], and [9], Greitzer model is presented with modifications.

Another alternative to deal with surge and improve the compression system's performance is to use advanced controlled techniques. Model Predictive Control (MPC) is an advanced control strategy successfully applied in the industry [10] which deals easily with constraints, multiple variables, and delays. MPC predicts the system's output through an explicit model of the system and calculates the control actions through the minimization of an objective function, considering the constraints of the system.

Control applications for centrifugal compressors are normally designed to deal with the fast dynamics of the machine. For advanced control systems based in MPC controllers, this imposes a constrain in the computational time, since the MPC would have to perform its calculations at a high sampling rate. MPC controllers have been applied to control centrifugal compressors at high sampling rate in [11], [12]. In [5] a MPC controller is designed to control the pressure and avoid to the surge. The minimization of the recycled gas is taken into account and the MPC is proposed as a replacement for the PID controllers of the regulatory control system.

Even though the MPC is considered to be able to replace multiple control loops with good results [13], in the compression system studied in this dissertation it is not possible to replace the regulatory system, given that the regulatory control loops are embedded in the compression system. For that, the proposed MPC has to work as a layer above the low level PID controllers.

The tunning of large scale MPC is a difficult problem and its solution relies on the knowledge of the processes and, oftentimes, in several try and error attempts. To overcome such problems, several

works proposed techniques to procedurally obtain the weights for the objective function [14, 15]

In this work, the satisficing approach presented in [16] was chosen. In this technique the weights are calculated on-line according to the operation point of the system, depending on which objective is further away from its goal. Considering the amount of variables and objectives, there are several possible combinations of weights that will determine the performance of the controlled system.

1.1 OBJECTIVES AND CONTRIBUTIONS

The objective of this dissertation is to present the application of an MPC controller designed to improve the compression system's performance, avoiding shut-down due to surge, and improving energy consumption. The centrifugal compression system of a particular off-shore oil and gas production platform is studied in this work. The MPC is implemented as a higher control level that runs at a low sampling rate (with sampling time equal to 5 seconds), above the PID regulatory control system. Even though the system can reach the surge point in less than 1 second, the MPC can still help the overall system's performance by anticipating actions to avoid surge and improving energetic efficiency.

The main contribution of this study is the modeling of a complete compression system, composed by two parallel 3-stage compression trains. The phenomenological model includes not only the typical modeling of a compression stage, but also the regulatory PID controllers, heat exchangers, vessels, the recycle lines and valves, and the exportation line.

Another contribution is the inclusion of the surge indexes as controlled variables so that they can be used for prediction and are affected by the manipulated variables. The index is easy to compute and takes into account the gas flow rate though the compressor and the minimum gas flow rate to avoid surge, calculated at every iteration based on the system's state.

Finally, a strategy to tune the controller is also proposed. The satisficing tuning technique is able to dynamically change the control tuning to prioritize the variables that are closer to violate their operation limits.

1.2 ORGANIZATION OF THE DISSERTATION

This dissertation is organized as follows: chapter 2 reviews the theory of Model Predictive Control (MPC), with emphasis in the recursive Dynamic Matrix Control (DMC), and presents a tuning technique implemented to improve the controller's performance.

Chapter 3 has a description of the compressor model and a discussion of the possible controlled and manipulated variables.

Chapter 4 details the implementation of the different solutions and the results. Finally, chapter 5 gives the conclusions.

2 MODEL PREDICTIVE CONTROL

This chapter presents an overview on MPC with its main concepts, with emphasis in the design of the DMC algorithm and the satisficing tuning technique, since they are used in this work.

Model predictive control is one of the most successful advanced control techniques applied in industry [10]. This success is due to the fact that MPC strategies can be applied to Single Input Single Output (SISO) and Multiple Inputs Multiple Outputs (MIMO) systems, with or without delay and constraints on outputs and control actions.

MPC is not limited to an unique control strategy. This name is used to designate a large group of control algorithms that:

- use an explicit model of the process to predict the system's behavior in a finite moving time horizon;
- calculate a sequence of future control actions through the minimization of an objective function.

The differences between the existent MPC algorithms rely on the different types of prediction and disturbance models, objective functions, and on the procedure to deal with the constraints and to obtain the control law.

Although there are several different MPC algorithms, they all have these three common elements:

- prediction model including a prediction error treatment method used to predict the systems behavior through a certain time period;
- objective function, which contains the control objective, for example tracking a reference or minimizing energy consumption;
- a procedure to obtain the control law, which minimizes the objective function.

The following section explains these elements in further details.

2.1 MPC ELEMENTS

2.1.1 Prediction model

The prediction model is in general given by a set of equations that models the input to output relation of the controlled system, but it could also be a fuzzy model or any other representation of the relation between the inputs, disturbances and outputs. The prediction model is an important element of the MPC strategy. As a general rule, the performance of MPC algorithms is connected to how well their underlying models can predict the plant input-output dynamics, therefore a good effort is put into defining prediction models that reflect reality as good as possible. The prediction error treatment method is different in every MPC algorithm.

The prediction model is composed by: the process model and the disturbances model. The predicted outputs of the system are then a combination of the outputs of the process model and the outputs of the disturbance model.

2.1.1.1 Process model

The process model defines the relation between the inputs and the outputs of the system. The model can be linear or nonlinear. The most common linear models are:

- impulse response;
- step response;
- transfer function;
- state space.

2.1.1.2 Disturbance model

The model for the disturbances is as important as the process model. The representation most widely used to describe deterministic and stochastic disturbances is known as Auto-Regressive Integrated Moving Average. This method models the differences between the model output and the process output as:

$$\eta(t) = \frac{C(z^{-1})e(t)}{D(z^{-1})}$$

where the polynomial $D(z^{-1})$ includes an integrator $\Delta = 1 - z^{-1}$, $e(t)$ is a white noise with average zero. The parameters of the polynomials C e D are used to describe the stochastic characteristics of η and the use of the integrator in D is very important in order to take into account step disturbances, which are very common in practice. This model can represent random changes, steady state off-sets, etc. This is the model used in GPC, EPSAC, EHAC, and in other controllers with a few modifications.

A particular case of disturbance model is the one used in the DMC algorithm, where the predicted disturbance $\hat{\eta}$ is considered constant and equal to the measured disturbance η, so $\hat{\eta}(t+k \mid t) = \eta(t)$ for all $k > 0$, and $e(t) = y(t) - \hat{y}(t)$ is the error between the process output $y(t)$ and the model output $\hat{y}(t)$. The computation of $\hat{y}(t)$ is presented in section 2.2.

Other representations of these models and the analysis of the effects the disturbance model has on the control system can be found in [17, 18].

2.1.1.3 Free and forced response

MPC with linear models consider the systems response to be a combination of two parts: the free response and the forced response. The idea is to consider the control sequence $u(t)$ as a superposition of two sequences:

$$u(t) = u_f(t) + u_c(t)$$

in which $u_f(t)$ corresponds to the past input values, that are kept constant in the future, that means:

$$\begin{aligned} u_f(t-j) &= u(t-j) \text{ for } j = 1, 2, \ldots \\ u_f(t+j) &= u(t-1) \text{ for } j = 0, 1, 2, \ldots \end{aligned}$$

and $u_c(t)$ corresponds to the future input values so they are equal to zero in the past and equal to the future control actions in the future:

$$\begin{aligned} u_c(t-j) &= 0 \text{ for } j = 1, 2, \ldots \\ u_c(t+j) &= u(t+j) - u(t-1) \text{ for } j = 0, 1, 2, \ldots \end{aligned}$$

The free response $y_f(t)$ is the output prediction when the input is equal to $u_f(t)$. The forced response $y_c(t)$ corresponds to the

predictions when the input is equal to $u_c(t)$. If a disturbance model is available, the free response may include the outputs of that model as well, so the predictions are as close to reality as possible.

2.1.2 Objective function

The objective function is chosen according to the control's purpose. In most cases the goal is to minimize the error between the predicted outputs $\hat{y}$ and their references y_r penalizing the control increments Δu. For a Single Input Single Output case, this results in the equation:

$$J = \sum_{j=N_1}^{N_2} \delta(j)[\hat{y}(t+j \mid t) - y_r(t+j)]^2 + \sum_{j=1}^{N_u} \lambda(j)[\Delta u(t+j-1)]^2 \quad (2.1)$$

where:

- N_1 and N_2 - minimum and maximum prediction horizon. They define the time window where it is desired that the output y follows the reference y_r. For example, the selection of a large N_1 implies that the mistakes on the first $N_1 - 1$ instants are not important and the obtained closed-loop response will tend to be smooth. In the case of systems with a delay d, the prediction horizon should start after d, so $N_1 > d$, since there will be no response from the system to input $u(t)$ until the instant $t = d$.
- N_u - control horizon. It defines the time window where it is important to limit the control action. Thus, the number of decision variables of the minimization problem is defined by N_u. Note that a bigger N_u implies in a more complex problem, on the other hand better responses can be obtained because of the bigger number of degrees of freedom. Usually, the control horizon is smaller than the prediction horizon, $N_u < N$, where $N = N_2 - N_1$. Practical experiments show that $N_u = N/5$ gives good results.
- $\delta(j)$ and $\lambda(j)$ - weights for error and control action. They are fundamental in the MPC formulation because they define which variables are more important in the cost function. These weighting sequences are often chosen constant or exponential over the horizon. For example, a function of the type $\delta(j) = \alpha^{N_2 - j}$ could be used so that the error penalization varies through the horizon.

Using the idea of forced and free responses to describe the predictions of the process output in the cost function, the prediction errors can be written as functions of the future control actions. Therefore, the future control movements can be computed minimizing J, as they are the only unknown variables of J.

2.1.2.1 Constraints

In practice, all processes are subject to constraints in both input and output variables. Examples of these constraints are the maximum and minimum limits of the actuators (e.g. valves), the maximum speed variation of a drive (e.g. servo drives) or the limits that can be achieved by the outputs of a system due to safety issues. In addition, there are economic objectives for the system operation that generally lead the controller to choose operating points at the limits. Thus, if the control actions are properly calculated for the system to work very close to the economic optimum point, the quality and cost of the production process are optimized [19]. For these reasons, it is important to consider the problem's constraints in the calculation of the control increments. The constraints are included to the optimization problem as a set of equations of type:

$$u_{min} \leq \quad u(t) \quad \leq u_{max} \quad \forall t \tag{2.2a}$$

$$\Delta u_{min} \leq \quad u(t) - u(t-1) \quad \leq \Delta u_{max} \quad \forall t \tag{2.2b}$$

$$y_{min} \leq \quad y(t) \quad \leq y_{max} \quad \forall t \tag{2.2c}$$

The MPC control action can be obtained at each sampling time solving a static optimization problem defined by:

$$\min_{\Delta \mathbf{u}} \quad J \tag{2.3a}$$

$$\text{subject to} \quad A\Delta\mathbf{u} < b \tag{2.3b}$$

where J is the objective function and A and b define the constraints 2.2.

For unconstrained problems, the solution that minimizes J can be obtained analytically, but for constrained problems it can not. In this case, solving J requires a much larger computational effort than in the unconstrained case. If J is a quadratic function and the constraints are linear, the constrained optimization problem defined in 2.3 can be solved by any standard/off-the-shelf quadratic programming solver. Despite the complexity of the calculation, the

MPC's ability to take restrictions into consideration is one of the reasons for its success in industrial applications.

In practice, there are several points to be carefully considered in the solution of a constrained MPC. The formulation of the problem should correctly define the constraints, and manage them when necessary. This management allows the correct operation of the optimization algorithm, releasing or smoothing the constraints, when possible. Also, from the point of view of the implementation of the optimization algorithm, is important to improve the efficiency and the minimization of computation times [20].

2.1.3 Control law

In every MPC algorithm the goal is to calculate $u(t+k \mid t)$, with $k = 0, 1, \ldots, N_u$. For this it is necessary to:

- calculate the predictions $\hat{y}(t+k \mid t)$ as a function of the future control increments;
- replace the predictions in the objective function J;
- calculate the control increments $\Delta\mathbf{u}$ that minimize J, considering the restrictions.

With these steps the future control increments in the control horizon are calculated. However, only the first increment is applied to the system.

2.1.4 Reference tracking and band control

One of the MPC's advantages is the possibility of using future references, when these values are available, to calculate the control signal. This allows the system to reach faster the desired new value. The values of $y_r(t+k)$ used in the objective function are not necessarily the actual system's reference. In practical applications, strategies to soften the reference changes are typically used. These strategies are similar to filters used in classical control structures with two degrees of freedom:

$$\begin{aligned} y_r(t) &= r(t) \\ y_r(t+k) &= \alpha y_r(t+k-1) + (1-\alpha) r(t+k) \end{aligned} \tag{2.4}$$

where α is a parameter between 0 and 1 and $k = 1, \ldots, N$. Equation 2.4 represents a first order low pass filter that can be adjusted to

smooth r more or less depending on the α value. These filters are commonly used in several MPC controllers, such as GPC and DMC.

Sometimes there is no reference $y_r(t)$ to track, but a range in which the controller has to keep the controlled variable y. The band is defined by a lower limit y_{min} and an upper limit y_{max}. To implement this band control, $y_r(t)$ is a decision variable of the optimization problem created to minimize the objective function J. If $y_{min} \leq y(t) \leq y_{max}$ then the solution is $y_r(t) = y(t)$, but if $y_{max} \leq y$ then $y_r(t) = y_{max}$ and if if $y \leq y_{min}$ then $y_r(t) = y_{min}$.

2.2 DYNAMIC MATRIX CONTROLLER (DMC)

The DMC is a well known MPC strategy, largely applied in refineries and chemical plants. A detailed description of the DMC can be found in the book of Camacho and Bordons [19], chapter 3. This section has a description of the modified DMC algorithm used in this work and proposed in [21].

DMC is a MPC strategy that can be applied for open-loop stable plants (and can be generalized for processes with integrator modes, but this case will not be considered here). The step response of the system is used to obtain the predictions:

$$\hat{y}(t+k|t) = \sum_{i=1}^{\infty} g_i \Delta u(t+k-i) + \eta(t+k|t) \tag{2.5}$$

where $\eta(t+k|t)$ is the prediction error in time $t+k$. This error is considered constant through the horizon. So $\eta(t+k|t) = \eta(t|t) = y(t) - y_o(t|t)$, where y_o is the prediction without corrections. Replacing the prediction error and rearranging equation 2.5 results in:

$$\begin{aligned} \hat{y}(t+k|t) = &\sum_{i=1}^{k} g_i \Delta u(t+k-i) + \sum_{i=1}^{\infty} g_{k+i} \Delta u(t-i) + y(t) \\ &- \sum_{i=1}^{\infty} g_i \Delta u(t-i) \end{aligned} \tag{2.6}$$

$$\begin{aligned} \hat{y}(t+k|t) = &\sum_{i=1}^{k} g_i \Delta u(t+k-i) \\ &+ \sum_{i=1}^{\infty} (g_{k+i} - g_i) \Delta u(t-i) + y(t) \end{aligned} \tag{2.7}$$

The infinite summation can be replaced by a M-terms summation because $g_{k+i} - g_i \cong 0, \forall i > M$, as the process is stable and the step response coefficients tends to a constant value. Now the prediction equation is:

$$\begin{aligned} \hat{y}(t+k|t) = \quad & \textstyle\sum_{i=1}^{k} g_i \Delta u(t+k-i) + \\ & \textstyle\sum_{i=1}^{M} (g_{k+i} - g_i) \Delta u(t-i) + y(t) \end{aligned} \tag{2.8}$$

Consider a prediction horizon N and a control horizon N_u, the predictions can be written in matrix form:

$$\hat{\mathbf{y}} = \mathbf{G}\ \mathbf{u} + I\Delta\mathbf{u}(t-1) + \mathbf{1}_N y(t) \tag{2.9}$$

where $\mathbf{1}_N$ is a $N \times 1$ vector of ones,

$$\mathbf{I}\Delta\mathbf{u}(t-1) = \begin{bmatrix} (g_2 - g_1) & (g_3 - g_2) & \dots & (g_{M+1} - g_M) \\ (g_3 - g_1) & (g_4 - g_2) & \dots & (g_{M+2} - g_M) \\ \vdots & \vdots & \dots & \vdots \\ (g_{N+1} - g_1) & (g_{N+2} - g_2) & \dots & (g_{N+M} - g_M) \end{bmatrix} \times \begin{bmatrix} \Delta u(t-1) \\ \Delta u(t-2) \\ \vdots \\ \Delta u(t-M) \end{bmatrix},$$

$$\mathbf{G}\mathbf{u} = \begin{bmatrix} g_1 & 0 & \dots & 0 \\ g_2 & g_1 & \dots & 0 \\ \vdots & \vdots & \dots & \vdots \\ g_N & g_{N-1} & \dots & g_{N-N_u} \end{bmatrix} \begin{bmatrix} \Delta u(t) \\ \Delta u(t+1) \\ \vdots \\ \Delta u(t+N_u-1) \end{bmatrix},$$

and $\hat{\mathbf{y}} = [\hat{y}(t+1|t), \dots, \hat{y}(t+N|t)]^T$. Note that in the computation of $\mathbf{G}$ and $\mathbf{I}$, $g_i = g_M$ if $i > M$.

Equation (2.9) can be rewritten as:

$$\hat{\mathbf{y}} = \mathbf{G}\mathbf{u} + \mathbf{f_r} \tag{2.10}$$

where $\mathbf{f_r} = \mathbf{I}\Delta\mathbf{u}(t-1) + \mathbf{1}_N y(t)$ is the system's free response as it only depends on the past values of the control action and process output.

From this equation, if the initial conditions are null then the free response is equal to zero. If an unit step is applied in u,

$$\Delta u(t) = 1, \Delta u(t+1) = 0, \cdots, \Delta u(t+N_u-1) = 0$$

the output $[\hat{y}(t+1), \hat{y}(t+2), \cdots, \hat{y}(t+N)]^T$ is equal do the first column of the matrix **G**. So, the first column of **G** can be obtained trough the systems step response.

Note that matrix **G** has dimension $N \times N_u$ and vector $\mathbf{u}$ dimension is $N_u \times 1$, although only $\Delta u(t)$ should be computed and used as the rest of the future control actions are discarded.

As shown in [19] and [22], the free response can be obtained recursively. The prediction for the instant $t+k$ can be obtained with the available information in t and $t-1$ given by:

$$y_o(t+k|t) = \sum_{i=k+1}^{\infty} g_i \Delta u(t+k-i)$$

$$y_o(t+k|t-1) = \sum_{i=k+2}^{\infty} g_i \Delta u(t+k-i)$$

The difference between them is only the control action $\Delta\mathbf{u}(t-1)$, which was not know at $t-1$. Hence, by subtracting one equation from the other:

$$\begin{aligned} y_o(t+k|t) - y_o(t+k|t-1) &= g_{k+1}\Delta u(t-1) \\ &\quad + \sum_{i=k+2}^{\infty} g_i \Delta u(t+k-i) \\ &\quad - \sum_{i=k+2}^{\infty} g_i \Delta u(t+k-i) \\ y_o(t+k|t) &= g_{k+1}\Delta u(t-1) + y_o(t+k|t-1) \end{aligned} \tag{2.11}$$

Therefore, at every iteration, before the DMC algorithm calculates the control increments, the prediction has to be updated with the latest known control action $\Delta u(t-1)$:

$$y_o = y_o + \begin{bmatrix} g_1 \\ g_2 \\ \vdots \\ g_M \end{bmatrix} \Delta u(t-1)$$

y_o is the vector with the prediction without considering the measured disturbances or corrections. Afterwards y_o is shifted in time to become a prediction from $t+1$ to $t+M$, whereas formerly it was a prediction from t to $t+M-1$. When the first element of the vector is discarded a new element has to be added at the end of the vector to keep y_o with size $M \times 1$. Considering that the process is stable:

$$\begin{aligned} y_o(t+M-1|t) &= \sum_{i=M}^{\infty} g_i \Delta u(t+M-1-i) \\ y_o(t+M|t) &= \sum_{i=M+1}^{\infty} g_i \Delta u(t+M-i) \\ &= \sum_{i=M}^{\infty} g_{i+1} \Delta u(t+M-1-i) \\ y_o(t+M|t) - y_o(t+M-1|t) &= \sum_{i=M}^{\infty} (g_{i+1}-g_i) \Delta u(t+M-1-i) \end{aligned}$$

Since $g_{i+1} - g_i \cong 0, \forall i > M$, we have $y_o(t+M|t) \cong y_o(t+M-1|t)$. So the shifted prediction $\mathbf{y}_o$ becomes:

$$\mathbf{y}_o = \begin{bmatrix} y_o(t+1|t) \\ y_o(t+2|t) \\ \vdots \\ y_o(t+M-1|t) \\ y_o(t+M-1|t) \end{bmatrix}$$

This recursive method simplifies the prediction calculations avoiding the need to keep track of the past values of $\Delta\mathbf{u}$. This method also facilitates the application of the prediction error treatment method presented in [21], where the authors proposed a filter to compute the non measured disturbances of the system. The prediction correction depends on the error between the measured output and the predicted one, and on the parameters of the filter:

$$c(t) = \beta c(t-1) + (1-\beta)(y(t) - y_o(t|t)) \tag{2.12}$$

where $c(t)$ is the prediction correction, β is the parameter of the filter, $y(t)$ is the measured output, $y_o(t|t)$ is the predicted output without correction.

Measured disturbances can also be included in the predictions if there is a model for the disturbance. Considering measured disturbances and prediction corrections, the free response becomes:

$$f_r = f_r + \begin{bmatrix} g_1 \\ g_2 \\ \vdots \\ g_M \end{bmatrix} \Delta u(t-1) + \begin{bmatrix} h_1 \\ h_2 \\ \vdots \\ h_M \end{bmatrix} \Delta w(t-1) + \mathbf{1}_M c(t)$$

where $[h_1\, h_2 \ldots h_M]$ are the coefficients of the step response of the disturbance model, Δw is the disturbance variation, and where $\mathbf{1}_M$ is a $M \times 1$ vector of ones.

2.3 MPC TUNING WITH SATISFICING TECHNIQUE

The function shown by equation 2.1 is a typical objective function used in SISO MPC algorithms and it has multiple objectives: the reference tracking $\delta(j)[\hat{y}(t+j \mid t) - y_r(t+j)]^2$ and the control actions penalization $\lambda(j)[\Delta u(t+j-1)]^2$. The weights for each objective λ and δ are usually determined by the control designer. These chosen values are usually fixed and determined based on the designer's knowledge about the process.

The satisficing MPC (SMPC) presented in [16] uses the satisficing theory to calculate the appropriate weights of the objective function for the current system's state.

The SMPC algorithm is a distributed MPC designed to attend the objectives and constraints of different local controllers. The solution to this distributed problem is the analytic center of the region that satisfies all the local controllers. This point is also the solution of the centralized problem with the equivalent weights in the objective function. In the SMPC the weights change according to the operation point, seeking a satisfactory tuning. The weights are calculated dynamically to give priority to the less satisfied local objectives. The satisfactory system's performance is obtained through the maximum value that an objective can add to the total objective function. So if an objective is close to its maximum value, the weight associate to it will be increased forcing the controller to give priority to this local objective. Satisficing tuning can be applied to any type of MPC controller that uses weights in the objective function.

The tuning procedure is explained below. Each objective has a satisficing factor called F_{sat} that is calculated based on the largest

contribution expected for the objective. For the reference tracking objective, for example, it is calculated as:

$$F_{sat} = \sum_{j=N_1}^{N_2} [e^*_{ref}(t+j \mid t)]^2 \tag{2.13}$$

where e^*_{ref} is the largest expected error between the reference and the predicted output $[\hat{y}(t+j \mid t) - y_r(t+j)]$, and N_1 and N_2 define the prediction horizon N.

For the control actions penalization F_{sat} can be calculated as:

$$F_{sat} = \sum_{j=1}^{N_u} [\Delta u^*(t+j-1)]^2 \tag{2.14}$$

where Δu^* is the largest expected control increment and N_u is the control horizon . The maximum contribution expected or tolerated for each objective is chosen by the control designer.

The main difference between the manual and the satisficing tuning is that in the first the chosen weights are usually kept constant and in the second they change given priority to the objectives that are closest to their limit F_{sat}.

The weight λ to be attributed to a term of the cost function at a given time instant is then calculated by:

$$\lambda = \frac{1}{F_{sat} - \bar{F}} \tag{2.15}$$

where F is the value of the objective at iteration k. The value of F can be calculated by equations 2.13 and 2.14 but instead of using the largest expected control action and reference error, the actual values of Δu and e_{ref} should be used. The weight is calculated through this procedure at every iteration.

When F approaches its satisficing factor ($F \to F_{sat}$), λ increases indefinitely ($\lambda \to \infty$). If F surpass F_{sat}, according to 2.15 $\lambda < 0$ which has no practical meaning. Thus, to avoid such problems, these critical conditions are tested before the weights are calculated. If one of these conditions is true, then the weight calculated on the previous iteration ($k-1$) is used, meaning that $\lambda_k = \lambda_{k-1}$.

It is important to highlight that the maximum values used to calculate F_{sat} are not boundaries. These are desired values, not operational constraints.

2.4 FINAL COMMENTS

This chapter presented an overview on MPC theory and its elements, highlighting the recursive DMC algorithm. These are important concepts that were used in the MPC formulations presented in chapter 4. Finally, the satisficing technique to tune the MPC controller was presented. This satisficing theory will be used in the proposed DMC of this dissertation, allowing the simplification of the tuning procedure. The next chapter presents the modeling of the compression system studied in this dissertation.

3 COMPRESSION SYSTEM

This chapter presents an overview of centrifugal compressors and its applications in off-shore oil and gas facilities. It also has a detailed description of the mathematical model used in the design of the MPC's prediction model and in the system simulations.

In production plants, compressors are the subsystems responsible for giving energy to the gas to increase its pressure, suppling a certain gas flow rate at a specific pressure according to the desired operating point and the specifications of the subsequent subsystem. Figure 3.1 was adapted from [1] and presents an offshore production platform with its main subsystems. The multiphase flow emanating from the wells is separated in three phases when it reaches the separator. The gas phase is directed to the compression system where its humidity, temperature, and pressure are changed to meet the operation requirements. The compressed gas can then be exported, used for gas-lift, used to generate energy, or return to the reservoir in injection wells.

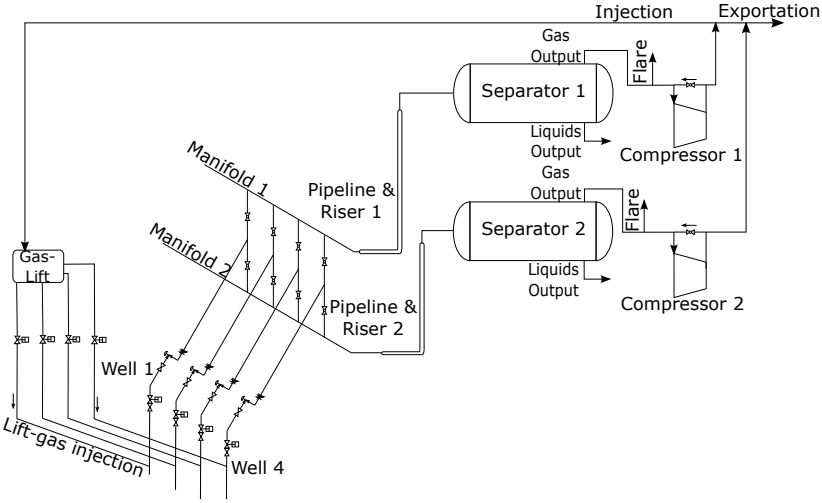

Figure 3.1: Production platform, adapted from [1]

The compression system has to process the gas flow rate delivered by the separator and if the compressor fails this gas accumulates causing the separator's pressure to rise. To prevent this pressure from exceeding safety limits, part of the uncompressed gas has to be flared. Another undesired situation is an inlet gas flow rate

below specified limits, which can take the compressor to an unstable region of operation. In this case, there can be a reverse gas flow inside the compressor that causes oscillations in the pressure and flow of the gas. This phenomenon is known as compressor surge [3][4].

The centrifugal compression system of a particular platform is studied in this work. A compression stage is made of two parts: the impeller and the diffuser. The gas is sucked through the center of the impeller and pushed by the centrifugal force to the diffuser, where the kinetic energy of the accelerated gas is then converted to pressure. The amount of energy a gas mass unit receives from the compressor is called head [3]. However not all the energy is used to increase the pressure. Due to friction and other irreversible losses, part of the energy is lost in the form of heat. Subsection 3.3.2 presents in more details the head calculation and its relation to the pressure increase.

For a compressor stage, the variables and parameters that define its performance are:

- p_s - suction pressure
- T_s - suction temperature
- p_d - discharge pressure
- MW - molecular weight of the gas mixture
- Z - gas compressibility
- k - gas specific heat ratio
- η_p - polytropic efficiency

These variables and parameters define the gas flow rate that the compressor is able to process and the amount of power required to achieve it. They also define the temperature of the compressed gas, or the discharge temperature T_d. Centrifugal compressors are designed to operate within a relatively small range of pressures, flows and gas characteristics. There are two phenomena that limit the operation of centrifugal compressors: stonewall or choke and surge. These phenomena, as well as the strategies to avoid them, are presented in section 3.1.

In this study the compression system consists in two parallel compressors with three stages each. A schematic of the system is

presented in figure 3.2. The two parallel compressor trains are connected to the inlet header at the entrance of the system and to an exportation header at the exit.

The pressures in the system are the inlet pressure p_{in}, the outlet pressure p_{out}, the discharge pressures pd_{ij}, where ij refers to the compression stage j of the compressor train i. The discharge pressure of one stage of compression is equal to the suction pressure of the next stage. The pressure ratio r is the relation between the discharge and the suction pressures of a certain stage and it represents how much the gas pressure has been increased. The gas mass flow rate entering and exiting the process are respectively m_{in} and m_{out}. The mass flow rate through the compressor is m and mass flow rate through the recycle valve is m_r.

The compression system also has PID controllers that are responsible for stabilizing the suction pressure, the discharge pressure, and the antisurge control. This regulatory layer was also modeled as part of the system so the prediction models would consider the influence of the PID controllers on the system. The MPC controller will not replace these PID controllers, but will work in a layer above the regulatory system to improve the systems performance.

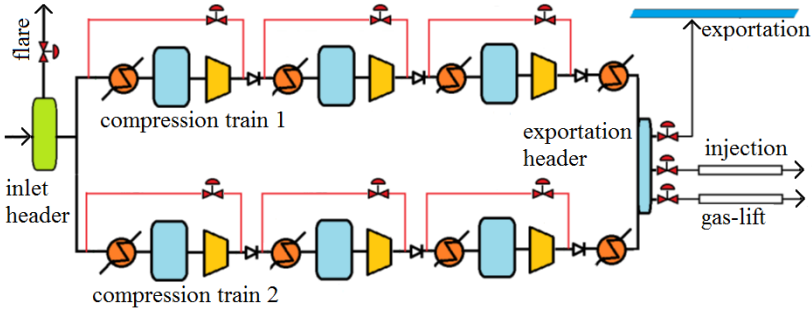

Figure 3.2: Compression system

3.1 SURGE AND STONEWALL

Surge is an unstable condition for the compressor operation that results in reverse gas flow rate though the compressor and fluctuations in the delivered pressure and flow rate [23, 6]. The surge phenomenon is associated with high pressure ratios and gas flow rates below the nominal flow rate of the compressor and thus con-

stitutes the lower boundary for stable flow rates. The occurrence of surge can severely damage the mechanical components of the compressor. It is important to determine the surge point so an antisurge controller can avoid surge by keeping the system operating in the stable operation region. Surge control in industrial applications still relies on preventing the surge occurrence [5]. For every pressure ratio and rotational speed there is a minimum volumetric flow rate, determined by the surge line, that guarantees the system's stable operation. In figure 3.3, the minimum flow is represented by point D. A well known antisurge control strategy is to use recycle valves to send part of the discharged compressed gas back to the suction to increase the flow through the compressor when necessary. Section 3.4.3 explains in further details the antisurge control system installed by the manufacturer in the compression system studied in this work. The compressor manufacturer, through a series of tests, determines the operation limits of the compressor stage. The surge and the stonewall or choke are the two phenomena that limit the compressor's operation and they are determined by the manufacturer. Figure 3.3, taken from [24], illustrates the relation between the volume flow rate Q and the pressure ratio r between the surge and stonewall limits. The compressor map for a real compressor does not define the points to the left of the surge line because the tests are not performed in the unstable region.

The stonewall phenomenon is associated with flow rates well above the nominal flow rate and it defines the upper boundary for stable flows. Stonewall is characterized by the occurrence of sonic speed in the compressor's impeller. It occurs when the system resistance decreases and flow increases. For a compressor of a single stage, the phenomenon happens when the head becomes null [24] and $r = 1$, which means the gas is flowing through the compressor without being compressed. The efficiency decreases due to increased energy losses in the form of heat. Some manufacturers limit the compressor's operation to the choke or stonewall region, but others allow their machine to operate in the choke region as long as the head is not negative [3].

.

3.2 SURGE INDEXES

The surge indexes are variables created to measure the distance between the current operation point and the surge line. In

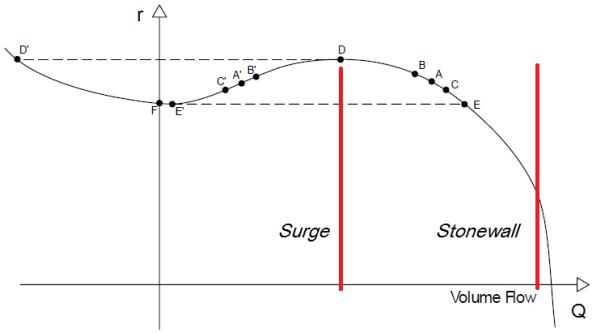

Figure 3.3: Surge and Stonewall

[25] a surge indicator that is not affected by the gas molecular weight is proposed. But the pressure drop on the orifice plate used to measure the volumetric gas flow has to be known and, for that, calculating this surge indicator in practice is difficult. In [13] a simpler surge index is presented as a performance indicator:

$$IS = \frac{Q_{surge}}{Q_{cp}} \tag{3.1}$$

where Q_{cp} is the volumetric flow rate of gas through the stage and Q_{surge} is the minimum volumetric flow that must go through that same stage to avoid surge at that operating point. The desired value for the index is $IS < 1$. The steps to calculate Q_{surge} are detailed in 3.3.1.

The IS values range from 0 to 1, where 1 means that the system went into surge. In this study IS is not only considered a performance indicator but also tested as a controlled variable for the MPC controllers discussed in chapter 4. Since the system has six stages, three for each compression train, the complete system has six indexes of surge, which are grouped in vector **IS**.

3.3 MODELING

The mathematical model of the compressor presented in this section is based on Greitzer [7]. Greitzer model is also used in [26], [4], [27], [28], [29], [24], [30] e [31].

The equations that define the dynamics of a compression stage were taken from [2]. The main equations are:

$$\frac{dp}{dt} = \frac{a_0^2}{V_p}(m - m_t) \tag{3.2}$$

$$\frac{dm}{dt} = \frac{A_1}{L_c}(\Psi(\omega, m)p_s - p_p) \tag{3.3}$$

$$\frac{d\omega}{dt} = \frac{1}{J}(\tau_d - \tau_c) \tag{3.4}$$

$$\tau_c = m\mu\omega r_2^2 \tag{3.5}$$

where:

a_0 - sonic velocity (m/s),

V_p - plenum volume (m^3),

A_1 - area of the impeller (m^2),

L_c - length of the duct (m),

$\Psi(\omega, m)$ - compressor characteristic curve,

J - compressor moment of inertia (kgm^2),

μ - compressor slip factor,

r_2 - impeller radius (m),

are the parameters and constants of the model and:

m - mass flow rate entering the plenum (kg/s),

m_t - mass flow rate through the throttle (kg/s),

p_s - suction pressure (Pa),

p_p - pressure in the plenum (Pa),

τ_d - driver torque (Nm),

τ_c - torque exerted by the compressor load (Nm),

ω - compressor speed (rad/s),

are the variables and states that change with time.

Figure 3.4 represents the model for a compression stage proposed by Gravdahl in [2]. In this work the model of the compression stage is slightly different, as the following simplifications were made:

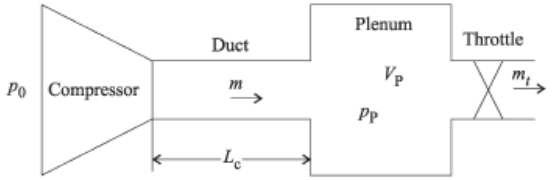

Figure 3.4: Compression stage configuration proposed in [2]

.

- there is no accumulation of gas in the compressor, so in equation 3.3 $\frac{dm}{dt} = 0$. This means $\Psi(\omega, m)p_0 = p_p$. This simplification relies on the fact that the variations on m with time inside the compressor would be very rapid and the use of the algebraic expression assumes an instantaneous change.

- it is assumed that the regulatory control system is part of the model.

- the compressor manufacturer data sheet is used to obtain the relation between discharge and suction pressure to the suction volumetric flow rate Q and compressor angular velocity ω, so $\Psi(\omega, Q) = p_p/p_s$.

- there is no mass exchange between gas and liquid phase in the scrubber.

- there is no energy losses in the heat exchanger. For the sake of control algorithms development this simplification is considered acceptable.

- there is no change in the gas compressibility with pressure. It is expected that Z changes would not lead to changes on the MPC algorithm choices.

The following subsections describe the equations used in this study. It is important to highlight that gas flow rates, pressures, temperatures, valve openings, and the rotational speeds of the two compression trains are states or algebraic variables of the model and they can change through time. The other elements of the model are constants and parameters.

3.3.1 Compression stage

In this work, each compression stage has the main compressor line and a recycle line with an antisurge valve used to prevent the occurrence of surge. In the main line there is a heat exchanger, a gas scrubber, and a compressor unit. The heat exchanger is responsible for keeping the gas temperature at the desired reference; the gas scrubber removes the gas condensate that forms because of the high pressure in the system; finally, the compressor unit is responsible for providing energy to the gas, increasing its pressure. Figure 3.5 shows the compression stage modeled in this section.

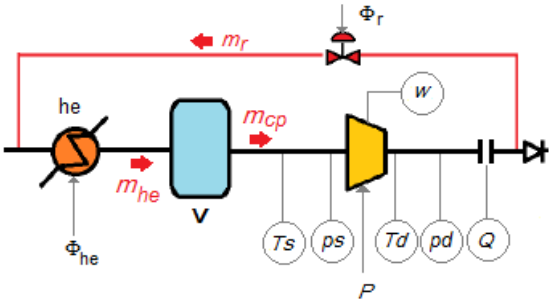

Figure 3.5: Compression stage modeled in this work

Each stage can be described by the same set of differential equations, therefore the next subsections present the modeling of the inlet header, of the outlet header, and of only one stage of compression. Since the three stages of each compression train are connected in series, the discharge pressure of one stage is equal to the suction pressure of the subsequent stage.

The original differential equations 3.2 to 3.5 do not include temperature changes caused by the heat exchanger or the dynamics of the recycled gas mass flow rate. So these equations were included in the model. In the model proposed in this study, the gas accumulation in the plenum is not considered. Instead $\frac{dp}{dt}$ is a function of the gas accumulation in the scrubber V (equation 3.2).

The compressor characteristic curve $\Psi(\omega, m)$ was obtained from the compressor map provided by the manufacturer. The map shows the relation between pressure ratio p_d/p_s, rotational speed ω, and gas flow rate m_{cp} through each compression stage. Besides, the map also shows the surge line, which represents the minimum flow

rate to avoid surge, given p_d/p_s and ω. An example of compression map is given in figure 3.8.

After the modifications and the addition of the heat exchanger and recycle loop dynamics, the set of equations 3.2 to 3.5 was changed. The new set of equations that represents a compression stage is:

$$\frac{dp_s}{dt} = \frac{ZRT_s}{MWV_s}(m_{he} - m_{cp}) \tag{3.6}$$

$$\frac{d\omega}{dt} = \frac{1}{J}(\tau_d - \tau_c) \tag{3.7}$$

$$\tau_c = \omega m_{cp} \mu r_2^2 \tag{3.8}$$

$$m_{he} = m_r + m_{in}^s \tag{3.9}$$

where:

Z - gas compressibility factor

MW - gas molecular weight (kg/mol)

R - gas constant (J/mol)

p_s - suction pressure of the stage (Pa)

T_s - suction temperature of the stage (K)

V_s - volume of the scrubber (m^3)

m_{he} - gas mass flow rate through the heat exchanger (kg/s)

m_{cp} - gas mass flow rate through the compressor unit (kg/s)

m_r - gas mass flow rate through the recycling line (kg/s)

m_{in}^s - gas mass flow rate that enters the stage (kg/s)

The discharge pressure of stage i is equal to the suction pressure of the subsequent stage $i+1$, so $p_{d,i} = p_{s,i+1}$, and p_s is determined by solving the differential equation 3.6 for each stage. The pressure ratio for each stage is $r_i = p_{d,i}/p_{s,i}$. From equation 3.3, considering $\frac{dm}{dt} = 0$, the pressure ratio is related to ω and m_{cp} by:

$$\Psi(\omega, m_{cp}) = \frac{p_d}{p_s} \tag{3.10}$$

In a compression stage, the relation between r, ω, and the volumetric flow rate Q_{cp} is given by the manufacture's compression map and can be approximated through a polynomial:

$$r = a + bx - cy - dx^2 + exy + fy^2 \tag{3.11}$$

with:

$$\begin{aligned} r &= \frac{p_d}{p_s} \\ y &= \frac{\omega}{\omega_{nom}} \\ x &= \frac{Q_{cp}}{y} \end{aligned}$$

where ω_{nom} is the compressor nominal rotational speed. Since, r and y are known, x is the one of the roots of 3.11. Figure 3.6 shows the relation between the volumetric flow rate and the pressure ratio for a few normalized rotational speeds. The surge line shown in the figure is where the pressure ratio is maximum and $dr/dQ = 0$. The surge volumetric flow Q_{surge} is Q at the point where $dr/dQ = 0$.

$$\begin{aligned} \frac{dr}{dQ} &= \frac{dr}{dx}\frac{dx}{dQ} \\ \frac{dr}{dQ} &= b\frac{dx}{dQ} + 2dx\frac{dx}{dQ} + ey\frac{dx}{dQ} \end{aligned} \tag{3.12}$$

Replacing $x = Q_{surge}/y$, $y = \omega/\omega_{nom}$, and $dx/dQ = 1/y$ in equation 3.12:

$$\begin{aligned} \frac{dr}{dQ} &= \frac{b}{y} + \frac{2d}{y}x + e = 0 \\ \frac{2d}{y^2}Q_{surge} &= -\frac{b}{y} - e \\ Q_{surge} &= \frac{-(by + ey^2)}{2d} \\ Q_{surge} &= \frac{-b\omega}{2d\omega_{nom}} + \frac{-e\omega^2}{2d\omega_{nom}^2} \end{aligned}$$

To simplify the calculations, Q_{surge} can be written as a functions of ω:

$$Q_{surge} = k_1\omega + k_2\omega^2$$
$$k_1 = \frac{-b}{2d\omega_{nom}}$$
$$k_2 = \frac{-e}{2d\omega_{nom}^2}$$

The manufacture's compression map does not show the system's behavior for the region where $dr/dQ < 0$, the part of the curve to the left of the surge line, because this is the unstable operation region and the system is not tested in these operation conditions. The compressor's stable operation region is to the right of the surge line. So x is the root of polynomial 3.11 that is to the right of the point where $dr/dQ = 0$.

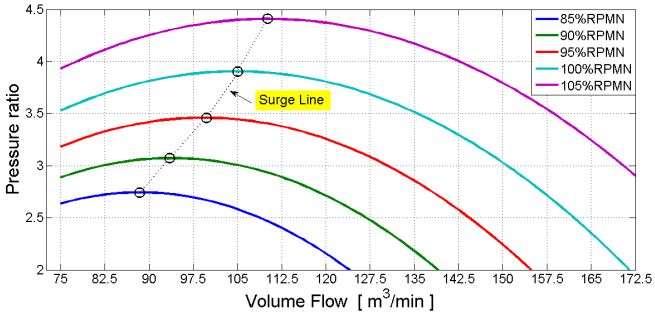

Figure 3.6: Relation between volumetric flow rate, pressure ratio, and normalized rotational speed

The gas volumetric flow rate Q_{cp} through the compressor is calculated from x, $Q_{cp} = xy$. The gas mass flow rate through a compressor stage m_{cp} depends of the gas density ρ:

$$m_{cp} = \rho Q_{cp} \tag{3.13}$$
$$\rho = \frac{MW}{ZRT_s} p_s \tag{3.14}$$

The recycled gas mass flow rate is computed using the equations for valves working with compressible fluids as recommended

by [32]:

$$m_r = N_{un} C V Y p_d \sqrt{\left(\frac{MWx}{ZRT_d}\right)} \tag{3.15}$$

$$CV = CV_N \Phi_r \tag{3.16}$$

$$F_k = \frac{k}{1.4} \tag{3.17}$$

$$x = min\left(\frac{p_d - p_s}{p_d}, F_k x_T\right) \tag{3.18}$$

$$Y = 1 - \frac{x}{3F_k x_T} \tag{3.19}$$

where:

m_r - gas mass flow rate through the recycling line (kg/s)

N_{un} - constant that converts the units

CV_N - flow coefficient

k - heat capacity ratio

The discharge temperature of the compressed gas can be obtained as:

$$T_d = T_s \left(\frac{p_d}{p_s}\right)^{\frac{k-1}{\eta_p k}}. \tag{3.20}$$

where:

η_p - polytropic efficiency

3.3.2 Power consumption

The head H is the amount of work per mass unit that has to be applied to the gas to compress it. According to [24], the energy balance in the compression can be expressed as:

$$H + dq = dh + \frac{c^2}{2} + gdz \tag{3.21}$$

where dq is the heat exchanged inside the impeller, dh is the variation of the gas enthalpy, $\frac{c^2}{2}$ is the kinetic energy of the gas, and gdz is the gravitational energy of the gas.

The process is considered to be adiabatic, so there is no heat exchange and $dq = 0$. The kinetic and gravitational energies are too small and can also be disregarded. So the head can be considered the energy required to change the enthalpy of the gas and it is given by:

$$H = dh \tag{3.22}$$

The enthalpy variation is:

$$dh = \frac{dp}{\rho} \tag{3.23}$$

where p is the gas pressure and ρ is the gas density.

Thus, the work per mass unit required to compress a gas from pressure p_1 to pressure p_2 can be obtained by:

$$H = \int_{p_1}^{p_2} \frac{dp}{\rho} \tag{3.24}$$

The gas density ρ can be expressed differently if the compression is isentropic, isothermal, or polytropic. The isentropic compression is adiabatic and reversible and the entropy is constant. The isothermal is also reversible and in this case the temperature remains constant. The polytropic compression is adiabatic but irreversible and in this case the efficiency of the compression is constant.

The polytropic compression is considered more appropriate according to [3]. In that case,

$$\frac{p}{\rho^n} = cte \tag{3.25}$$

$$\rho = \rho_1 \left(\frac{p}{p_1}\right)^{1/n} \tag{3.26}$$

n is the polytropic exponent. Replacing equation 3.26 in 3.24:

$$H = \frac{p_1^{1/n}}{\rho_1} \int_{p_1}^{p_2} \frac{dp}{p^{1/n}} \tag{3.27}$$

After solving the integral in equation 3.27, the head equation becomes:

$$H = \frac{p_1^{1/n}}{\rho_1} \left(\frac{p^{\frac{-1}{n}+1}}{\frac{-1}{n}+1} \right) \Bigg|_{p=p_1}^{p_2}$$

with

$$\rho_1 = \frac{p_1 MW}{Z_1 R T_1} \tag{3.28}$$

where MW is the gas molecular weight, Z_1 is the gas compressibility at point 1, and T_1 is the gas temperature at point 1. Replacing equation 3.28 in 3.3.2 gives:

$$H = \frac{Z_1 R T_1}{MW} \frac{n}{n-1} \left[\left(\frac{p_2}{p_1} \right)^{\frac{n-1}{n}} - 1 \right]. \tag{3.29}$$

The polytropic exponent n can be expressed in therms of the polytropic efficiency η_p and the gas specific heat ratio k:

$$\frac{n-1}{n} \approx \frac{k-1}{\eta_p k} \tag{3.30}$$

The polytropic efficiency η_p is also calculated from a polynomial obtained from the compressor's manufacturers data sheet.

Thus, the equation for the head becomes:

$$H = \frac{Z_1 R T_1}{MW} \frac{\eta_p k}{k-1} \left[\left(\frac{p_2}{p_1} \right)^{\frac{k-1}{\eta_p k}} - 1 \right]. \tag{3.31}$$

The absorbed compressor power P is given by:

$$P = \frac{m_{cp} H}{\eta_p} \tag{3.32}$$

where m_{cp} is the gas mass flow rate going through the compressor.

3.3.3 Inlet header

The inlet header is represented by a compressor inlet drum with volume V_{in}, shown in figure 3.7.

The gas phase from the separator reaches the compression system with a mass flow rate m_{in}. From the inlet header, the gas mass flow rate is divided between the two compression trains. Connected to this vessel is also the flare line with a flare valve. This valve opens releasing gas to the flare if the pressure in the inlet header p_{in} reaches its maximum limit. The pressure p_{in} depends on

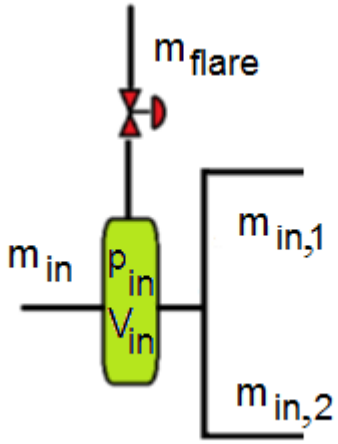

Figure 3.7: Inlet header

the mass balance in the vessel.

$$\frac{dp_{in}}{dt} = \frac{RZT_{in}}{MWV_{in}}(m_{in} - m_{in,1} - m_{in,2} - m_{flare}) \tag{3.33}$$

$$m_{in,1} = k_{he}^{1}\sqrt{\frac{MW}{ZRT_{in}}}\sqrt{p_{in}(p_{in} - p_{s}^{1})} \tag{3.34}$$

$$m_{in,2} = k_{he}^{2}\sqrt{\frac{MW}{ZRT_{in}}}\sqrt{p_{in}(p_{in} - p_{s}^{2})} \tag{3.35}$$

where:

p_{in} - pressure in the inlet header

V_{in} - volume of the compressor inlet drum

T_{in} - temperature of the gas entering the compression system

m_{in} - gas mass flow rate entering the compression system

$m_{in,1}$ - gas mass flow rate entering the compression train 1

$m_{in,2}$ - gas mass flow rate entering the compression train 2

m_{flare} - gas mass flow rate in the flare line

$p_{s,1}$ - suction pressure of stage 1 of compression train 1

$p_{s,2}$ - suction pressure of stage 1 of compression train 2

In equations 3.34 and 3.35, $k_{he,1}$ and $k_{he,2}$ are constants that represent the pressure drop in the heat exchanges 1 e 2.

3.3.4 Outlet header

The dynamics of the outlet header pressure p_{out} is obtained from the mass balance:

$$\frac{dp_{out}}{dt} = \frac{ZRT^h}{MWV_h}(m_{out,1} + m_{out,2} - m_{exp} - m_{p1} - m_{p2}) \quad (3.36)$$

Where:

V_h - outlet header volume, it represents the total volume associated with the pipes.

$m_{out,1}$ - gas mass flow rate from compressor train 1,

$m_{out,2}$ - gas mass flow rate from compressor train 2,

m_{exp} - gas mass flow rate delivered the exportation line,

m_{p1} - gas mass flow rate delivered to process 1,

m_{p2} - gas mass flow rate delivered to process 2.

The modeling of the pressure in the exportation line was simplified to avoid the use of partial differential equations. The pressure was modeled as a combination of pressure loss and pressure variation due to the gas accumulation in the line. It is assumed that in the export line there is a gas flow m_{ext} which is independent. Furthermore it is assumed that in the steady state $m^d_{exp} = m_{exp}$ and that this transition has a first order dynamic. The pressure p_{exp} is then written as:

$$p_{exp} = p_{exp,1} + p_{exp,2} \quad (3.37)$$

$$\frac{dm^d_{exp}}{dt} = -\frac{m^d_{exp}}{\sigma^m_{exp}} + \frac{m_{exp}}{\sigma^m_{exp}} \quad (3.38)$$

$$p^2_{exp} = k_{exp,1}(m^d_{exp} + m_{ext})^2 \quad (3.39)$$

$$\frac{dp_{exp,1}}{dt} = K^d_{exp}\left(m_{exp} - m^d_{exp}\right) \quad (3.40)$$

$$K^d_{exp} = \frac{ZRT^h}{MWV_{lexp}} \quad (3.41)$$

where:

σ_{exp}^{m} - time constant,

$k_{exp,1}$ - constant that depends on the length and diameter of the export line, the friction factor, and the average pressure through the line,

V_{lexp} - volume of the exportation line.

3.4 REGULATORY CONTROL

The regulatory control system is formed by PID controllers and it was also modeled as part of the compression system. Every PID has an anti-windup. The regulatory control system considered in the compressor modeling presented in this dissertation is composed by:

1. Inlet gas pressure and load sharing control
2. Outlet gas pressure and exportation flow control
3. Antisurge control
4. Suction temperature control

3.4.1 Inlet pressure and load sharing

The compressor inlet pressure p_{in} depends on the mass balance of the vessel V_{in}, shown in equation 3.33.

The manipulation of $m_{in,1}$ and $m_{in,2}$ can take p_{in} to the desired value. The flows $m_{in,1}$ and $m_{in,2}$ depend on the rotational speed of the compressor w, which depends on the power P applied

to the compressor. The control law for p_{in} is given by:

$$e_{pin} = -p_{in}^{sp} + p_{in} \tag{3.42}$$

$$u_{pin,1} = Kp_{pin}e_{pin} + Ki_{pin}\int_0^t e_{pin}(\tau)d\tau + u_{bias,1} \tag{3.43}$$

$$u_{pin,2} = Kp_{pin}e_{pin} + Ki_{pin}\int_0^t e_{pin}(\tau)d\tau + u_{bias,2} \tag{3.44}$$

$$u_{bias,1} = Kp_{bias}e_{dsm,1} + Ki_{bias}\int_0^t e_{dsm,1}(\tau)d\tau \tag{3.45}$$

$$u_{bias,2} = Kp_{bias}e_{dsm,2} + Ki_{bias}\int_0^t e_{dsm,2}(\tau)d\tau \tag{3.46}$$

$$e_{dsm,1} = d_{surge}^{mean} - d_{surge,1} \tag{3.47}$$

$$e_{dsm,2} = d_{surge}^{mean} - d_{surge,2} \tag{3.48}$$

$$d_{surge,1} = Q_1 - Q_{surge,1} \tag{3.49}$$

$$d_{surge,2} = Q_2 - Q_{surge,2} \tag{3.50}$$

$$d_{surge}^{mean} = \frac{d_{surge,1} + d_{surge,2}}{2} \tag{3.51}$$

where:

e_{pin} - error between the setpoint and p_{in},

p_{in}^{sp} - setpoint for p_{in},

Kp_{pin} - proportional gain of the inlet pressure controller,

Ki_{pin} - integral gain of the inlet pressure controller

Kp_{bias} - proportional gain of the load sharing controller,

Ki_{bias} - integral gain of the load sharing controller

Q_1 and Q_2 - volumetric flow rate through the first stage of compressor train 1 and 2, respectively

$Q_{surge,1}$ and $Q_{surge,2}$ - surge volumetric flow rate for the first stage of compressor train 1 and 2, respectively

The terms $u_{bias,1}$ and $u_{bias,2}$ implement the load sharing, so that both compressor trains are always at the same distance of the surge point.

3.4.2 Outlet header pressure

The outlet header pressure p_{out} depends on the mass balance $m_{out,1} + m_{out,2} - m_{exp} - m_{p1} - m_{p2}$, as shown in equation 3.36. The gas flow rate directed to the exportation line m_{exp} is regulated by the exportation valve opening ϕ_{exp}. The pressure p_{out} can be changed by manipulating ϕ_{exp}. The control law for ϕ_{exp} is given by:

$$e_{pout} = p_{out}^{sp} - p_{out} \tag{3.52}$$
$$\phi_{exp} = -Kc_{exp} * e_{pout} - Ki_{exp} \int_0^t e_{pout}(\tau) d\tau$$

where:

e_{pout} - error between the setpoint and p_{out},

p_{out}^{sp} - setpoint for p_{out},

Kp_{exp} - proportional gain of the outlet pressure controller,

Ki_{exp} - integral gain of the outlet pressure controller

3.4.3 Antisurge control

Compressor data sheets are usually provided by the compressor manufacturer. They contain important information on the compressor's behavior and operating points. Figure 3.8 shows a typical compressor map taken from a compressor's data sheet. The graph shows the relation between the volumetric flow rate at compressor's suction and the pressure ratio for different rotational speeds. In the map, the red solid line is known as the surge line. As explained in section 3.1, this line defines the minimum flow required to avoid surge, Q_{surge}. Anti surge control techniques usually consider a safer surge line, called control surge line or safe surge line, represented by the blue dashed line on the graph. Commonly, the control surge line is the surge line plus a slack of $5 - 10\%$ of the minimum flow rate.

If the compressor is working at a point to the left of the safe surge line then the flow rate through the compressor is below the minimum. Recycling part of the compressed gas can increase the gas flow through the compressor, preventing the system to go into surge. And if the compressor is working at a point to the right of the safe surge line, no action is required.

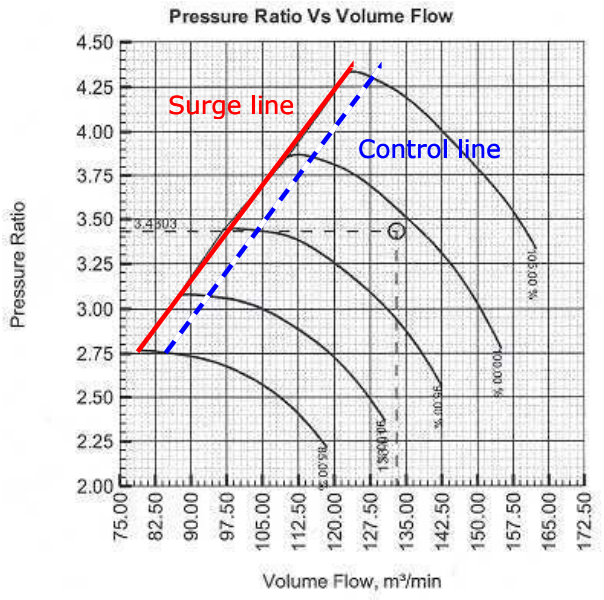

Figure 3.8: Example of a compressor map

So the antisurge control of this system consists on opening a recycle valve allowing part of the discharged compressed gas to go back to compressor suction. This will increase the compressor's gas flow keeping it above the minimum and avoiding surge.

The minimum flow obtained through the control surge line Q_{surge} is used to define the setpoint for the PI controller Q^{sp}_{surge} as shown in equation 3.53.

$$Q^{sp}_{surge} = Q_{surge}(1 + slack) \tag{3.53}$$

For each stage there is an antisurge recycling valve. The valve opening, ϕ_r is determined by the control law in equation 3.55.

$$e_s = Q^{sp}_{surge} - Q \tag{3.54}$$

$$\Phi_r = Kp_r e_s + Ki_r \int_0^t e_s(\tau) d\tau \tag{3.55}$$

where:

Q - flow through the compressor stage,

Kp_r - proportional gain of the PI controller,

Ki_r - integral gain of the PI controller,

3.4.4 Suction temperature control

On the suction of each compression stage there is a heat exchanger that keeps the suction temperature at a desired value. The gas temperature control is based on the coolant flow.

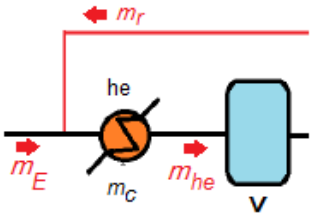

Figure 3.9: Gas flows through the heat exchanger

Figure 3.9 shows the important flows used in the modeling of the temperature control where:

m_E - gas mass flow from inlet header or from the previous stage,

m_r - recycled gas mass flow,

m_{he} - gas mass flow trough the heat exchanger,

m_c - coolant mas flow,

The amount of energy in the heat exchanger is given by W_{in}:

$$W_{in} = m_r c_g T_d + m_E c_g T_E + \Phi_{he} m_c^{max} c_c T_c. \tag{3.56}$$

where:

T_E - inlet gas temperature,

T_d - discharge gas temperature (same as the temperature of the recycled gas),

T_s - suction gas temperature,

T_c - coolant temperature,

c_g - gas specific heat,

c_c - coolant specific heat,

Φ_{he} - heat exchanger valve opening.

In steady state the coolant and the gas temperatures are considered the same since the modeling assumes no heat losses:

$$W_{out} = (m_{he}c_g + \Phi_{he}m_c^{max}c_c)T_s^{ss} \tag{3.57}$$

Considering no energy loss, $W_{in} = W_{out}$ and

$$T_s^{ss} = \left(m_R c_g T_d + m_E c_g T_E + \Phi_{he} m_c^{max} c_c T_C\right) / (m_{TC} c_g + \Phi_{he} m_c^{max} c_C). \tag{3.58}$$

Assuming a first order dynamics, the suction temperature's differential equation T_s is:

$$\frac{dT_s}{dt} = -\frac{T_s}{\sigma_{Ts}} + \frac{T_s^{ss}}{\sigma_{Ts}} \tag{3.59}$$

The heat exchanger's valve opening Φ_{he} is given the control law in equation 3.61:

$$e_{Ts} = T_s^{sp} - T_s \tag{3.60}$$

$$\Phi_{he} = Kp_{Ts}e_{Ts} + Ki_{Ts}\int_0^t e_{Ts}(\tau)d\tau \tag{3.61}$$

3.5 SYSTEM SIMULATION

This section analyses the system's behavior without the MPC layer. Here only the regulatory control is active. This results will be the base for comparison of the proposed MPC controllers in the next chapters. The two compressor trains are identical so only the results of one the trains are shown in this section.

The compression system nonlinear model described in section 3.3 was implemented in Matlab and the differential equations were solved with ODE45. For the simulations and comparisons a simple scenario was chosen, where the inlet flow varies as illustrated in figure 3.10. This input flow is the main disturbance applied to the system to create the scenario. The simulation starts with the flow on its nominal value. Then the flow drops by 50%. This drives the system to the surge region. After the drop, the inflow rises to 115% of its nominal value, forcing the system to flare gas. The results of the regulatory controlled system are shown in figures 3.11 to 3.17.

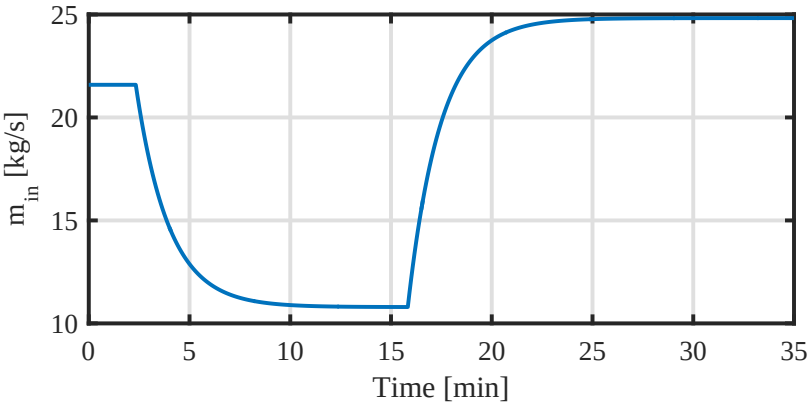

Figure 3.10: Inlet gas flow

Figure 3.11 shows that the inlet pressure controller is able to keep p_{in} at its setpoint $p_{in}^{sp} = 6.2$ when m_{in} is low, but when m_{in} is higher than the compressor's capacity, the rotational speed reaches its maximum limit and p_{in} increases. When p_{in} reaches the relief valve pressure limit, the flare valve opens and allowing gas to flow to the flaring system, as can be seen in figure 3.12.

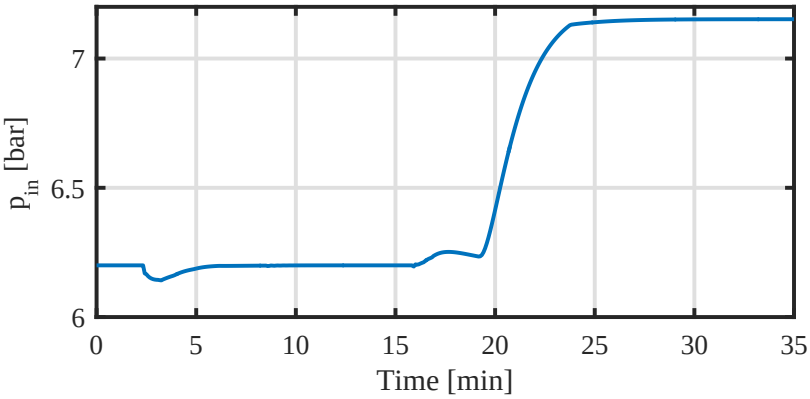

Figure 3.11: Results of the regulatory control system - inlet header pressure

Figures 3.13 to 3.15 show the surge indexes and the antisurge valves openings. As m_{in} decreases the surge indexes increase. When

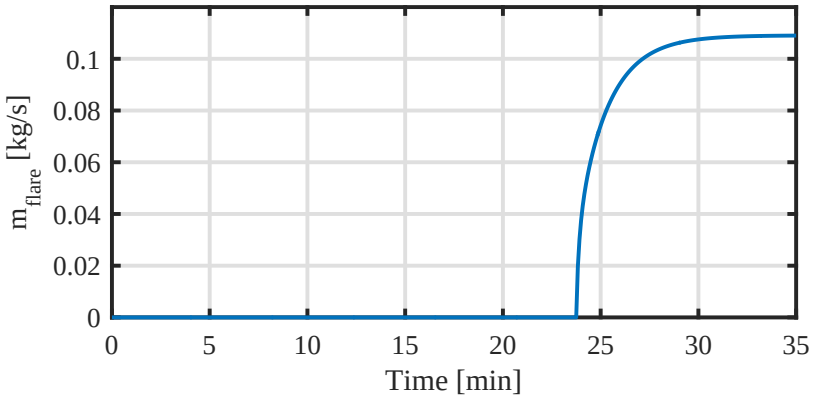

Figure 3.12: Results of the regulatory control system - flared gas

they reach 0.95 the antisurge valves open to increase the gas flow through the compressor and avoid surge. But m_{in} keeps decreasing and, when $\phi_{ASV,1}$ is totally opened, stage 1 starts to approach the surge region. Figure 3.13 shows that the antisurge valve of stage 1 saturates. When $IS_1 = 1$ the compressor is surging. If one stage goes into surge the system shuts down even if the other stages are not surging.

Figure 3.16 shows the outlet header pressure p_{out}. The regulatory control keeps it at its setpoint $p_{out}^{sp} = 176$. Figure 3.17 show that the consumed power decreases when m_{in} is low and increases almost to its maximum when m_{in} increases.

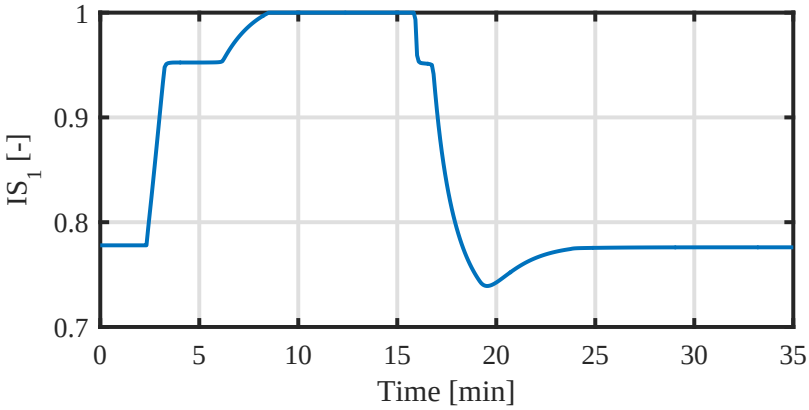

(a) Surge index

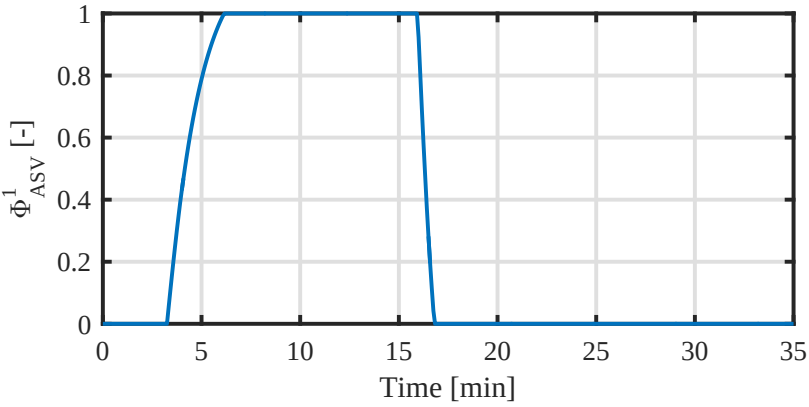

(b) Antisurge valve opening

Figure 3.13: Results of the regulatory control system - Stage 1

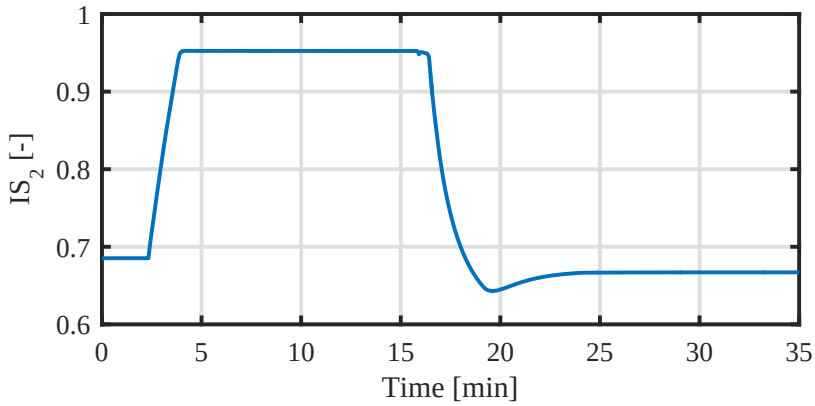

(a) Surge index

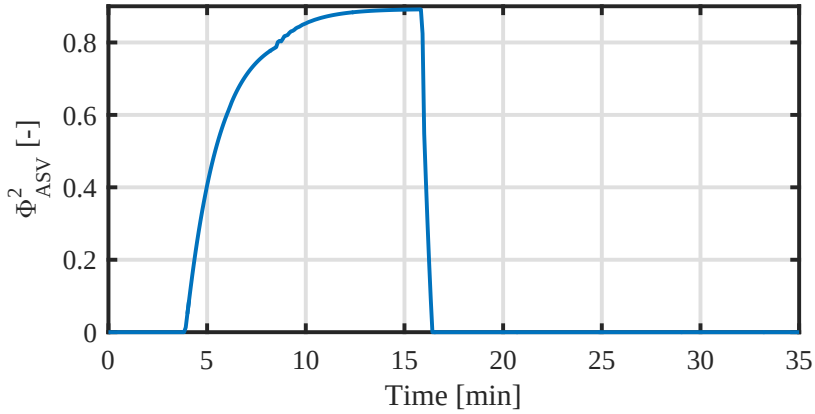

(b) Antisurge valve opening

Figure 3.14: Results of the regulatory control system - Stage 2

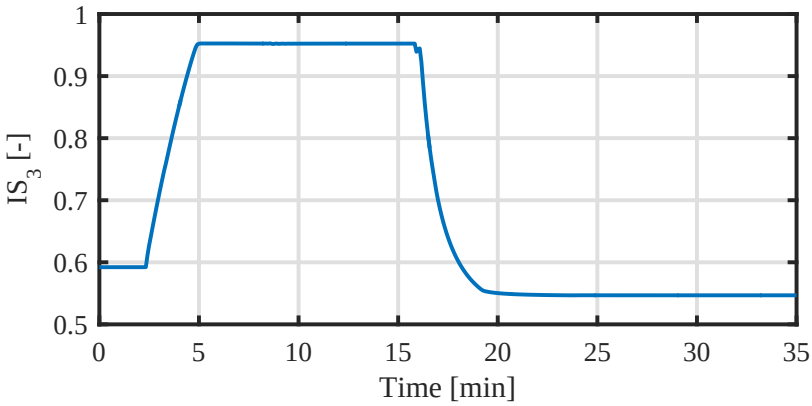

(a) Surge index

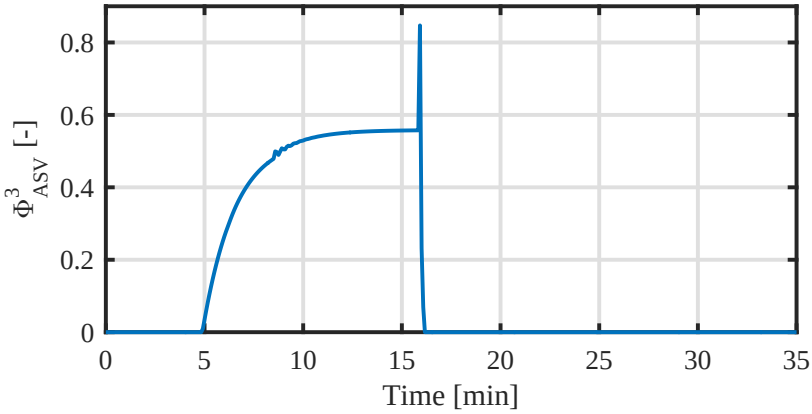

(b) Antisurge valve opening

Figure 3.15: Results of the regulatory control system - Stage 3

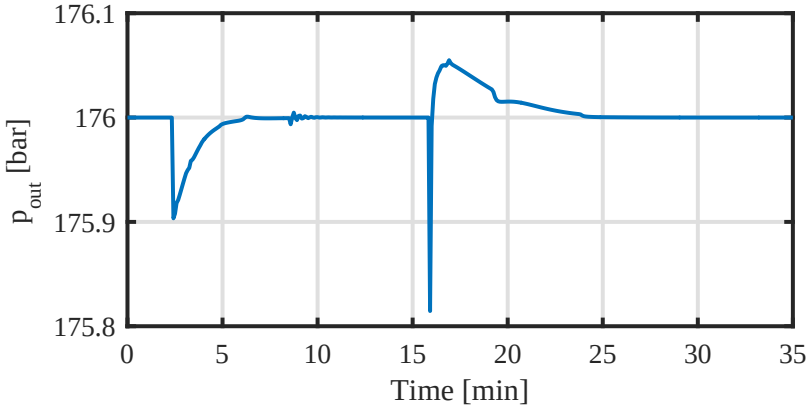

Figure 3.16: Results of the regulatory control system - outlet header pressure

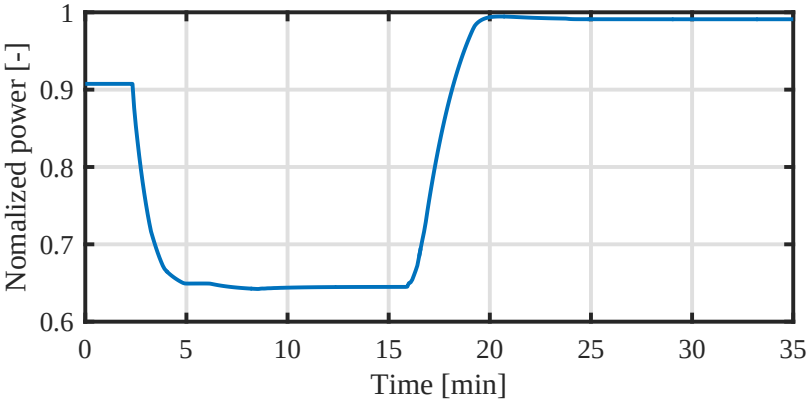

Figure 3.17: Power consumption

The simulated scenario shows that for a gas inflow drop of 50% this system would go into surge. A real compression system would stop working if it went into surge. So, the system's behavior observed when $IS = 1$ is not real. However, this simulation shows that, for this m_{in} disturbance, the regulatory control was not able to avoid surge. Based on that, an advanced control algorithm could be implemented to improve the compression system's performance.

3.6 CONTROL OBJECTIVES

The MPC designed for the compression system has these control objectives:

- To avoid surge and system's shutdown increasing the Mean Time Between Failure (MTBF) of the compressor system
- To minimize gas flaring
- To minimize energy consumption

The setpoints for the regulatory control could be used as manipulated variables for the MPC controller. The antisurge PID controller allows another signal to override its output, sending a different signal to the antisurge valve. So the antisurge valve openings could also be manipulated variables.

To avoid the occurrence of surge, the surge indexes could be used as controlled variables. The compressors energy consumption E could be expressed as a component of the control objective function J. The compressors energy consumption can be expressed as the sum of the integral of the power along the prediction horizon for each compressor.

$$E = \sum_{j=1}^{2} E_j \tag{3.62}$$

$$E_j = \int_{to}^{to+N} P_j(t)dt \tag{3.63}$$

Besides these objectives, the suction and discharge pressures of each stage have to be kept within their operation limits. They could also be included as controlled variables or as constraints for the optimization problem that calculates the control increments.

3.7 LINEAR MODEL

The nonlinear model of the compression system, including the regulatory control, is given by a set of algebraic and differential equations. The outputs y of the system are a function of the states x and the control signals u. This relation is represented by equation 3.64.

$$y = f(x, u) \tag{3.64}$$

In [33] the Practical Non Linear MPC (PNMPC) is introduced. In this work the author shows that the matrix **G** used by the MPC may be obtained from the Jacobian matrix of the system:

$$\mathbf{G} = \left[\frac{\partial f}{\partial u}\right] = \begin{bmatrix} \frac{\partial f(t+1|t)}{\partial u(t)} & 0 & \cdots & 0 \\ \frac{\partial f(t+2|t)}{\partial u(t)} & \frac{\partial f(t+2|t)}{\partial u(t+1)} & \cdots & 0 \\ \vdots & \vdots & \ddots & \vdots \\ \frac{\partial f(t+N|t)}{\partial u(t)} & \frac{\partial f(t+N|t)}{\partial u(t+1)} & \cdots & \frac{\partial f(t+N|t)}{\partial u(t+N-1)} \end{bmatrix} \tag{3.65}$$

If the system is considered to be time-invariant, then **G** can be approximated to:

$$\mathbf{G} = \left[\frac{\partial f}{\partial u}\right] = \begin{bmatrix} \frac{\partial f(t+1|t)}{\partial u(t)} & 0 & \cdots & 0 \\ \frac{\partial f(t+2|t)}{\partial u(t)} & \frac{\partial f(t+1|t)}{\partial u(t)} & \cdots & 0 \\ \vdots & \vdots & \ddots & \vdots \\ \frac{\partial f(t+N|t)}{\partial u(t)} & \frac{\partial f(t+N-1|t)}{\partial u(t)} & \cdots & \frac{\partial f(t+1|t)}{\partial u(t)} \end{bmatrix} \tag{3.66}$$

Thus, for a linear system as well as for a linearized representation [34], the matrix **G** is equivalent to the one built in the DMC controller algorithm. The first column of the matrix **G** is the step response of the system and it is also used to calculate the free response. The vector with the step response coefficients g can be obtained by:

$$g = \frac{f(\bar{x}, \bar{u} + \Delta u) - f(\bar{x}, \bar{u})}{\Delta u} \tag{3.67}$$

where $(\bar{x}, \bar{u})$ is the point where the function is linearized. In this study, the system was linearized off-line at an equilibrium point that corresponds to the system's steady state x_{ss} and u_{ss}. So, $\bar{x} = x_{ss}$ and $\bar{u} = u_{ss}$. The same linearized models were used through the entire simulations.

3.7.1 Step responses analysis

Instead of the coefficients of the step responses normally used in linear MPC control systems, the coefficients obtained using the

PNMPC technique were used here. For a linear system these coefficients would be identical to the ones obtained with the application of a step [33]. However for a nonlinear system the PNMPC coefficients correspond to the coefficients of the linearized system. For simplicity, these coefficients will be called step responses. This subsection presents the analysis of these linear models so the most adequate variables can be selected to be used by the MPC controller.

Considering the setpoints and manipulations that can be changed in the compression system regulatory system, the possible manipulated variables are:

- u_1 - setpoint of the inlet gas pressure (p_{in}^{sp})
- u_2 - setpoint of the outlet gas pressure (p_{out}^{sp})
- u_3 - opening of the antisurge valve of stage 11 ($\phi_{ASV,11}$)
- u_4 - opening of the antisurge valve of stage 12 ($\phi_{ASV,12}$)
- u_5 - opening of the antisurge valve of stage 13 ($\phi_{ASV,13}$)
- u_6 - opening of the antisurge valve of stage 21 ($\phi_{ASV,21}$)
- u_7 - opening of the antisurge valve of stage 22 ($\phi_{ASV,22}$)
- u_8 - opening of the antisurge valve of stage 23 ($\phi_{ASV,23}$)

Based on the control objectives described in section 3.6, the possible controlled variables are:

- y_1 - discharge pressure of stage 11 (pd_{11})
- y_2 - discharge pressure of stage 12 (pd_{12})
- y_3 - discharge pressure of stage 21 (pd_{21})
- y_4 - discharge pressure of stage 22 (pd_{22})
- y_5 - surge index of stage 11 (IS_{11})
- y_6 - surge index of stage 12 (IS_{12})
- y_7 - surge index of stage 13 (IS_{13})
- y_8 - surge index of stage 21 (IS_{21})
- y_9 - surge index of stage 22 (IS_{22})

- y_{10} - surge index of stage 23 (IS_{23})
- y_{11} - consumed power (P)

The step responses coefficients were normalized by:

$$\mathbf{sr}_{nm}^{norm} = \mathbf{sr}_{nm} \frac{range_u^m}{y_{nom}^n} \times 100\% \tag{3.68}$$

where $\mathbf{sr}_{nm}$ is the vector with the step response coefficients between the controlled variable n and the manipulated variable m, $range_u^m$ is the range of the manipulated variable m, and y_{nom}^n is the nominal value of the controlled variable n. Thus, $\mathbf{sr}_{nm}^{norm}$ shows the percentage variation of n in relation to its nominal value, for a variation in m.

Figures 3.18 to 3.21 show the step responses between the possible manipulated variables u and the possible controlled variables y. The coefficients of the step responses were normalized by equation 3.68. The inter stage discharge pressures p_d ($y1$ to $y4$), shown in figure 3.18, are highly sensitive to changes in $u1$ and $u2$. But $y1$ and $y3$ are linearly dependent of $y2$ and $y4$ respectively. Besides, if $u1$ and $u2$ are kept within their limits, $y1$ to $y4$ also stay within their limits. So instead of using them as controlled variables, their lower and upper limits were included in the problem's constraints to be safe. The indexes of surge IS ($y5$ to $y10$), shown in figures 3.19 and 3.20, are highly influenced by changes in the antisurge valve openings ($u3$ to $u8$). The consumed power P ($y11$), shown in figure 3.21, is influenced by all the manipulated variables. The gain between $u1$ and P is negative while the gain between the rest of the manipulated variables and P is positive. These results suggest that, at this operating point, P could be minimized if $u1$ is maximized while $u2$ to $u8$ are minimized.

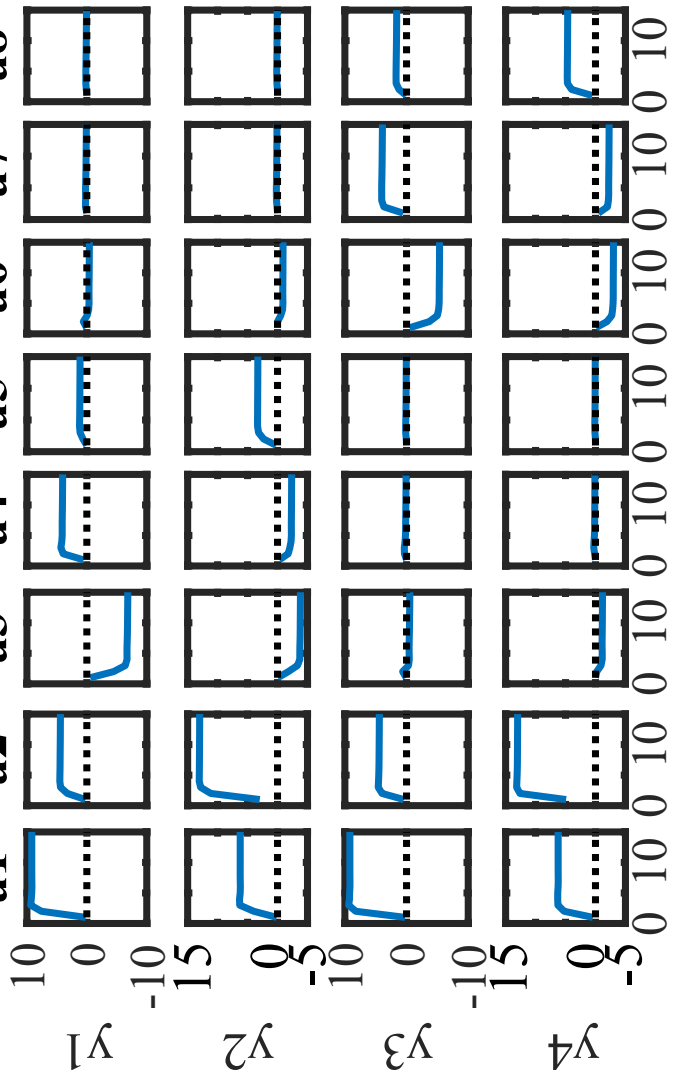

Figure 3.18: Matrix of the step responses between the possible manipulated and controlled variables

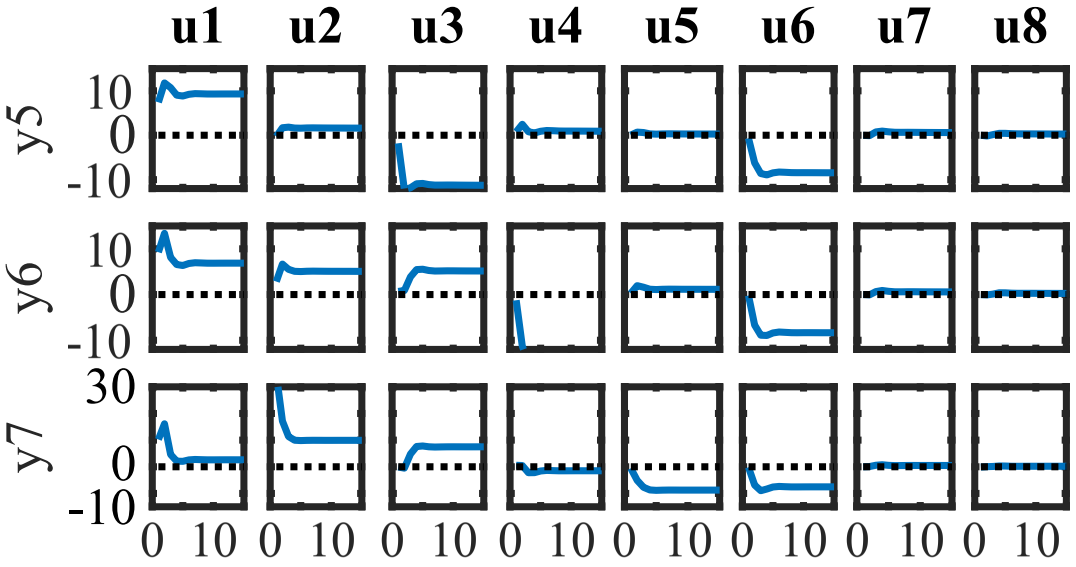

Figure 3.19: Matrix of the step responses between the possible manipulated and controlled variables

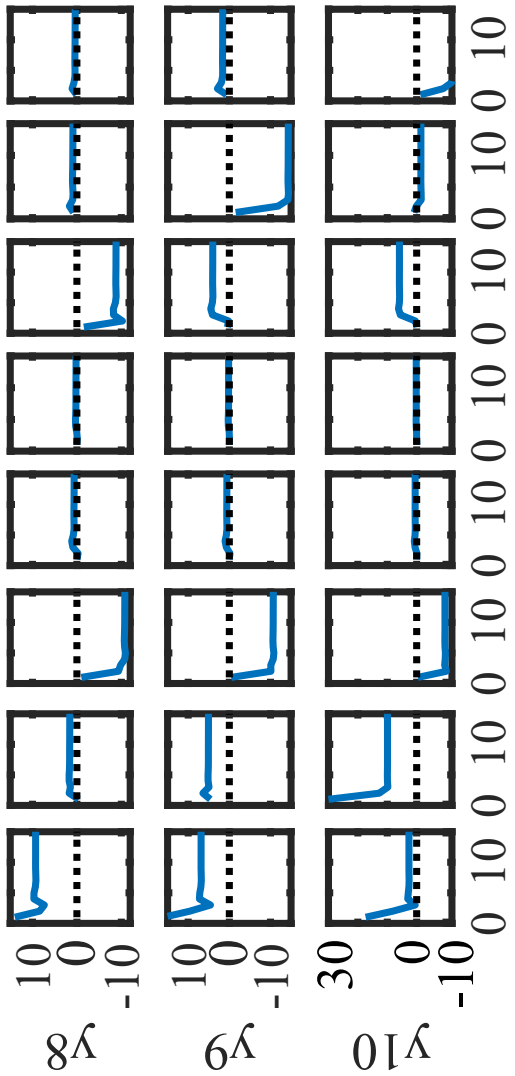

Figure 3.20: Matrix of the step responses between the possible manipulated and controlled variables

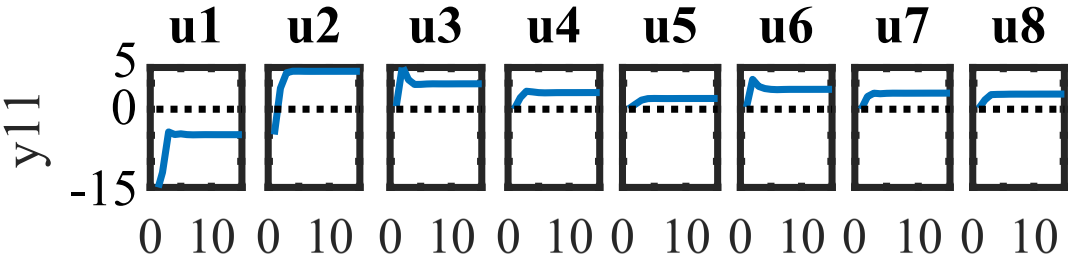

Figure 3.21: Matrix of the step responses between the possible manipulated and controlled variables

The relation between P and p_{in} is particularly interesting. There is a direct relation between the gas mass flow rate m_{cp} and consumed power P, meaning that an increase on m_{cp} implies in the greater consumption of power. At the same time there is a direct relation between the head H and P. Since the head depends on the pressure ratio $r = p_d/p_s$ and assuming a fixed discharge pressure p_d, it is possible to conclude that there is an inverse relation between the suction pressure p_s and the consumed power P. That is, if the suction pressure is increased, less power is required in the compression process.

$$P = \frac{m_{cp}H}{\eta_p} \tag{3.69}$$

$$H = \frac{Z_1 R T_1}{MW} \frac{\eta_p k}{k-1} \left[\left(\frac{p_d}{p_s} \right)^{\frac{k-1}{\eta_p k}} - 1 \right]. \tag{3.70}$$

When the compressor is not recycling, the static gain between p_s and P is negative. In this situation, changes in the pressure will not result in changes in the gas mass flow through the compressor. But when the compressor is recycling gas to avoid surge, a reduction in p_s moves the system away from the surge region, which leads to a reduction on the recycled gas flow m_r and consequently on the flow through the compressor m_{cp}. As explained before, a reduction in m_{cp} leads to a reduction in power consumption. So, if there is gas recirculation, the static gain between p_s and P could become positive.

Figure 3.22 shows the static relation between p_{in}, P, and ϕ^1_{ASV}. These values were obtained for a low gas flow rate, when the compression system is forced to recycle gas to avoid surge. The dashed blue line represents the relation between p_{in} and the anti-surge valve opening of the first stage ϕ^1_{ASV} in steady state. In this situation, smaller values of p_{in} require smaller ϕ^1_{ASV} to avoid surge. The solid red line represents the relation between p_{in} and the consumed power P. In this situation the gain between these variables changes signal. For this reason, including the model for $p_{in} \times P$ in the prediction model of the MPC could decrease the system's performance instead of improving it.

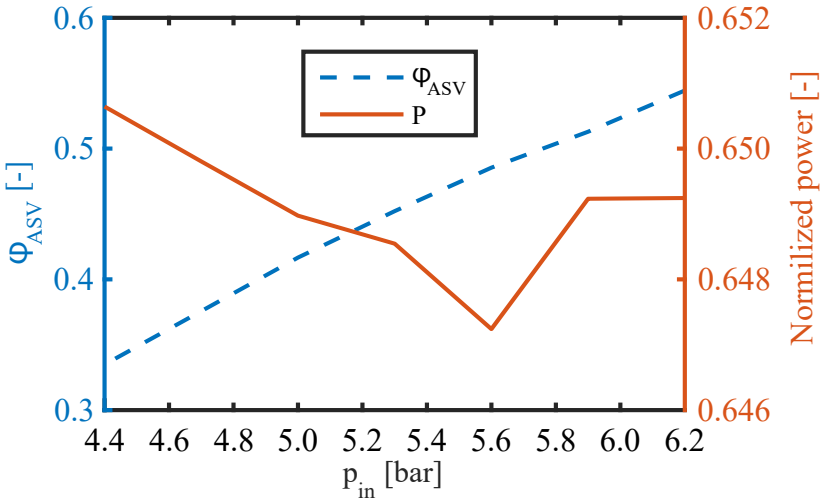

Figure 3.22: Static relation between p_{in}, P, and $\phi_{ASV,1}$

3.7.2 Variables selection

Considering the step responses analysis presented in 3.7.1, and which setpoints and valve openings can be changed in the compression system regulatory system, the possible manipulated variables are:

- p_{in}^{sp} - setpoint of the inlet gas pressure
- p_{out}^{sp} - setpoint of the outlet gas pressure
- $\phi_{ASV,11}$ - opening of the antisurge valve of stage 11
- $\phi_{ASV,12}$ - opening of the antisurge valve of stage 12
- $\phi_{ASV,13}$ - opening of the antisurge valve of stage 13
- $\phi_{ASV,21}$ - opening of the antisurge valve of stage 21
- $\phi_{ASV,22}$ - opening of the antisurge valve of stage 22
- $\phi_{ASV,23}$ - opening of the antisurge valve of stage 23

Based on the control objectives described in section 3.6, the possible controlled variables are:

- IS_{11} - surge index of stage 11

- IS_{12} - surge index of stage 12
- IS_{13} - surge index of stage 13
- IS_{21} - surge index of stage 21
- IS_{22} - surge index of stage 22
- IS_{23} - surge index of stage 23

Besides these variables, the energy consumption E could be included as an additional objective in the objective function to guarantee energy minimization.

The energy consumption depends on the power consumed by the compression system. As explained before, the static gain between p_{in} and P changes with the operation point. Changes in the signal of static gains can be difficult for the linear MPC algorithm to correct and the controller could not work properly.

3.8 FINAL COMMENTS

This chapter described the compression system studied in this dissertation, with a detailed description of the system's mathematical model. This nonlinear model was used to simulate the system and to study its behavior. This model, that is one of the contributions of this work, was published in [25, 35].

This chapter also presented an analysis of the potential controlled and manipulated variables to be used by the MPC controllers to achieve the control objectives. Based on the variables selection, the linearized prediction models were then obtained from the nonlinear model.

Next chapter presents two MPC controllers. In the first one, the manipulated variables are driven to values that minimize the power consumption. The total energy is then minimized indirectly. In the second formulation, the energy consumption is minimized directly in the objective function. This requires a linear model to express the dynamics between the manipulated variables and energy consumption

4 IMPLEMENTATION AND RESULTS

This chapter presents the two different MPC configurations that were tested to achieve the control objectives and improve the compression system's performance. The results were also compared with the system controlled by the regulatory layer only. The MPC controller implemented for this study is a recursive DMC controller with a correction filter like the one proposed in [21].

The MPC controller is implemented as a layer above the low-level or regulatory control, formed by the PID controllers, as illustrated in figure 4.1.

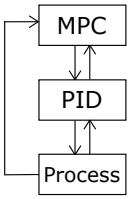

Figure 4.1: MPC and PID interaction

These experiments were also implemented in Matlab and the differential equations were solved with ODE45. The sampling time for the MPC controller is 5s. The process was simulated using the complete non-linear model of the plant described in section 3.3.

Each MPC has a set of controlled variables, henceforth called y, and manipulated variables, henceforth called u. The selection of these variables was based on the control objective defined for the compression system, and system analysis presented on chapter 3.

As explained before, the control actions are $\mathbf{u}_k = \mathbf{u}_{k-1} + \Delta\mathbf{u}_k$ and the increments $\Delta\mathbf{u}_k$ are obtained through the minimization of a cost function subject to constraints.

The MPC controllers studied in this dissertation have different objective functions and tuning strategies. Section 4.1 has a detailed explanation of the MPC implementations tested in the scenario with no additional modeling errors. The results of the application of both MPC formulations were very similar, but only MPC2 could be improved by a more appropriated tuning of the controller. In section 4.2 a robustness test is presented. In the test, modeling errors were introduced and only the second MPC implementation was considered robust.

4.1 MPC IMPLEMENTATIONS

The MPC controllers exposed in this section are variations of the DMC algorithm, as explained in section 2.2. The first MPC implemented (section 4.1.1) does not consider the energy consumption directly in its formulation due to its very nonlinear relation with the manipulated variables. The energy consumption was included in the second MPC formulation (section 4.1.2). As this process has variables with very different dynamics and amplitudes, tuning the MPC is not straightforward. Hence, in section 4.1.3 the satisficing tuning technique was applied to the MPC2 formulation to obtain more appropriate weights. The application of the technique led to a improved controller performance. The results were also compared against the system controlled only with the PID controllers. This comparison is carried out in the same scenario explained in section 3, where the gas flow rate that enters the compression system was used to disturb the plant's behavior. Figure 4.2 represents the changes in the gas flow rate m_{in} during the simulation. The flow starts at 21.5857 kg/s, then it drops to 50% of the initial value, causing the system to go into surge without a proper control strategy. After that the flow rises to 115% of its initial value, causing the input pressure to go above its maximum limit, that can cause the flare of part of the entering gas.

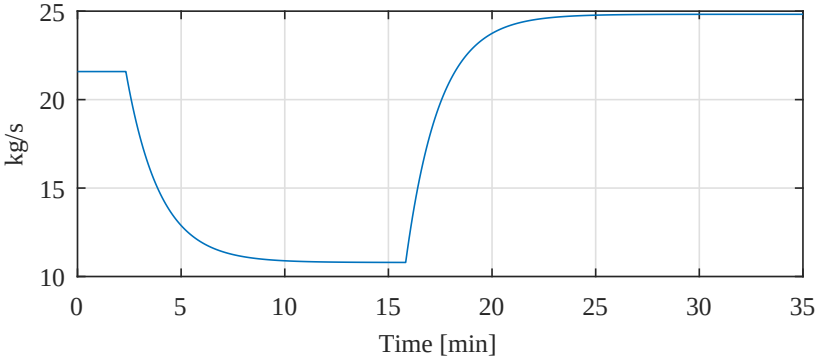

Figure 4.2: Gas flow rate that enters the compression system - m_{in}

The controlled and manipulated variables, the objective function, and the constraints were chosen based on the compression system analysis presented in chapter 3 and are described for each controller in the following sections.

4.1.1 MPC 1

The energy consumption can be minimized if p_{in} is maximized and p_{out} and m_r are minimized. For this compression system it is easy to determine the ideal values for the manipulated variables that guarantee energy saving. So, instead of considering the consumed energy as a term in the control objective function, this first MPC was designed to drive the manipulated variables to their ideal values whenever possible. With this formulation, it is not necessary to include the model that relates the power with the manipulated variables, so the controller will not have to deal with its nonlinearities.

Controlled and manipulated variables

To achieve the control objectives the MPC1 controlled variables (y) are:

- y_1: surge index of stage 11 (IS_{11})
- y_2: surge index of stage 12 (IS_{12})
- y_3: surge index of stage 13 (IS_{13})
- y_4: surge index of stage 21 (IS_{21})
- y_5: surge index of stage 22 (IS_{22})
- y_6: surge index of stage 23 (IS_{23})

To keep these variables controlled, the MPC1 manipulated variables (u), are:

- u_1: setpoint of the inlet gas pressure (Pin_{sp})
- u_2: setpoint of the outlet gas pressure ($Pout_{sp}$)
- u_3: opening of the antisurge valve of stage 11 ($\phi_{ASV,11}$)
- u_4: opening of the antisurge valve of stage 12 ($\phi_{ASV,12}$)
- u_5: opening of the antisurge valve of stage 13 ($\phi_{ASV,13}$)
- u_6: opening of the antisurge valve of stage 21 ($\phi_{ASV,21}$)
- u_7: opening of the antisurge valve of stage 22 ($\phi_{ASV,22}$)
- u_8: opening of the antisurge valve of stage 23 ($\phi_{ASV,23}$)

Thus, MPC1 sends setpoints to the inlet pressure PID controller and to the outlet pressure PID controller, and defines the position of the antisurge valves.

Objective function

The objective of this formulation, J (equation 4.1), is to bring the control variables $\mathbf{y}$ to their references $\mathbf{y}_r$ and the manipulated variables $\mathbf{u}$ to their targets $\mathbf{u}_t$ while minimizing the control variation $\Delta\mathbf{u}$.

$$J = [\hat{\mathbf{y}} - \mathbf{y}_r]^T \mathbf{Q}_y [\hat{\mathbf{y}} - \mathbf{y}_r] + \Delta\mathbf{u}^T \mathbf{Q}_u \Delta\mathbf{u} + [\mathbf{u} - \mathbf{u}_t]^T \mathbf{Q}_t [\mathbf{u} - \mathbf{u}_t] \quad (4.1)$$

Control tuning

The diagonal matrices $\mathbf{Q}_y$,$\mathbf{Q}_u$, and $\mathbf{Q}_t$ are formed respectively by the weights defined for reference error, target error, and control variation. These weights were chosen manually:

$$\mathbf{Q}_y = diag([10, 10, 10, 10, 10, 10])$$

$$\mathbf{Q}_u = diag([0.1, 0.1, 1, 1, 1, 1, 1, 1])$$

$$\mathbf{Q}_t = diag([0.01, 0.01, 0.1, 0.1, 0.1, 0.1, 0.1, 0.1])$$

These values were chosen so that the reference error was the first priority and the target error the last priority in the objective function minimization. It is important to highlight that $\hat{\mathbf{y}}$ are kept in a band, as explained is section 2.1.4.

Constraints

The problem's constraints are defined in 4.2. There are lower and upper boundaries for manipulated and controlled variables, $\mathbf{u}$ and $\mathbf{y}$. The control increment $\Delta\mathbf{u}$ is also limited, so the changes in the control actions are smooth.

$$\Delta\mathbf{u}_{min} \leq \Delta\mathbf{u} \leq \Delta\mathbf{u}_{max} \quad (4.2a)$$

$$\mathbf{u}_{min} \leq \mathbf{u} \leq \mathbf{u}_{max} \quad (4.2b)$$

$$\hat{\mathbf{y}}_{min} \leq \hat{\mathbf{y}} \leq \hat{\mathbf{y}}_{max} \quad (4.2c)$$

$$(4.2d)$$

The boundaries for the controlled variables are:

$$
\begin{aligned}
0 \leq y_1 \leq 0.93 \\
0 \leq y_2 \leq 0.93 \\
0 \leq y_3 \leq 0.93 \\
0 \leq y_4 \leq 0.93 \\
0 \leq y_5 \leq 0.93 \\
0 \leq y_6 \leq 0.93
\end{aligned}
$$

The boundaries for the manipulated variables are:

$$
\begin{aligned}
5.27 \leq u_1 \leq 6.2 \\
160 \leq u_2 \leq 200 \\
\Phi r_{reg,11} \leq u_3 \leq 1 \\
\Phi r_{reg,12} \leq u_4 \leq 1 \\
\Phi r_{reg,13} \leq u_5 \leq 1 \\
\Phi r_{reg,21} \leq u_6 \leq 1 \\
\Phi r_{reg,22} \leq u_7 \leq 1 \\
\Phi r_{reg,23} \leq u_8 \leq 1
\end{aligned}
$$

The lower boundaries for the positions of the antisurge valves change at every iteration. The MPC has to calculate a valve opening that is greater than the one defined by the regulatory control system so $u_{min} = \Phi r_{reg}$. This ensures that the MPC will never close the valves if the regulatory system decides to open them, condition that can violate the compressor manufacturer's warranty.

Results

Figures 4.3 to 4.8 show the results of the application of MPC1 in the simulated scenario presented in figure 4.2. In the figures, the dashed black lines represent the system's performance with the regulatory system only and the blue solid lines are the results of the application of the MPC1 controller. In figures 4.3a, 4.4a, and 4.5a the doted black lines are the maximum limit of the surge indexes. The results show that MPC1 was able to prevent the system to go into surge, since the indexes never reach the value 1, even when the gas flow rate is at its minimum. But MPC1 was not able to keep the indexes below their upper limit in the steady state. This problem could be solved by selecting a more appropriate set of tuning values.

If the weights for this objective were greater, the indexes might be kept below 0.93. However, when this was tried, the control actions were too aggressive, which suggested that other weights should be changed. The results presented in this section are the best ones obtained by manual tuning. In this solution 22 weights have to be selected to tune the controller. Tuning a MIMO MPC is always difficult, and the manual procedure is not simple. Before studying an improved method for MPC tuning, a different formulation is analyzed. So the next solution includes the energy consumption directly in the objective function and only the target for u_1 is kept. The number of weights that have to be selected was then reduced, facilitating the tuning.

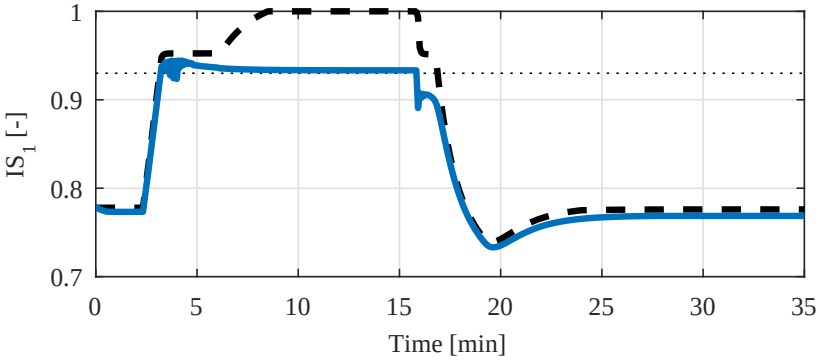

(a) Surge index

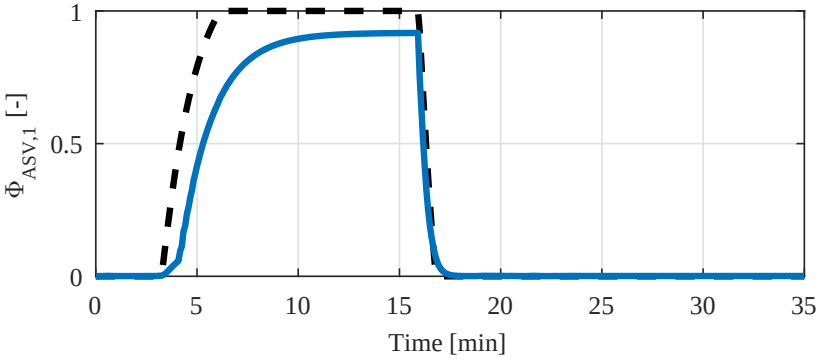

(b) Antisurge valve opening

Figure 4.3: Results of the application of MPC1 - Stage 1. Dashed black line: regulatory control without MPC, solid blue line: regulatory control with MPC1, doted black line: surge index upper limit

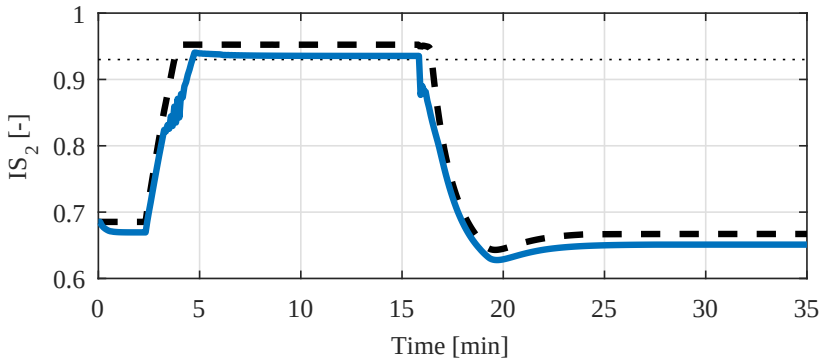

(a) Surge index

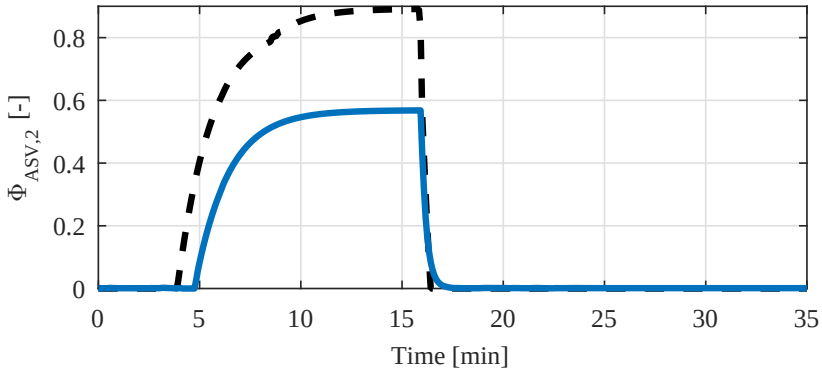

(b) Antisurge valve opening

Figure 4.4: Results of the application of MPC1 - Stage 2. Dashed black line: regulatory control without MPC, solid blue line: regulatory control with MPC1, doted black line: surge index upper limit

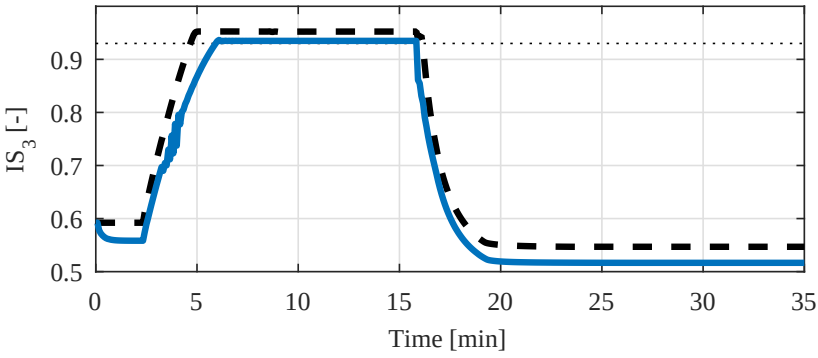

(a) Surge index

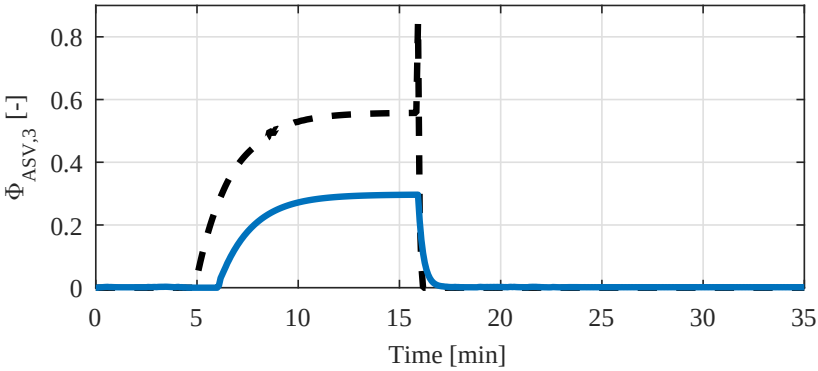

(b) Antisurge valve opening

Figure 4.5: Results of the application of MPC1 - Stage 3. Dashed black line: regulatory control without MPC, solid blue line: regulatory control with MPC1, doted black line: surge index upper limit

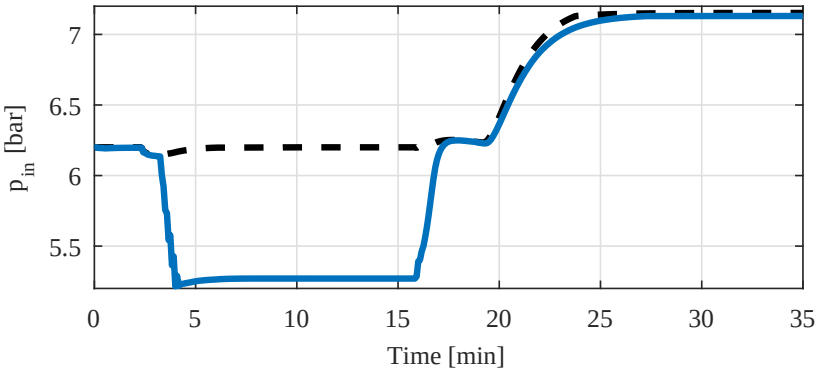

Figure 4.6: Results of the application of MPC1 - inlet header pressure. Dashed black line: regulatory control without MPC, solid blue line: regulatory control with MPC1

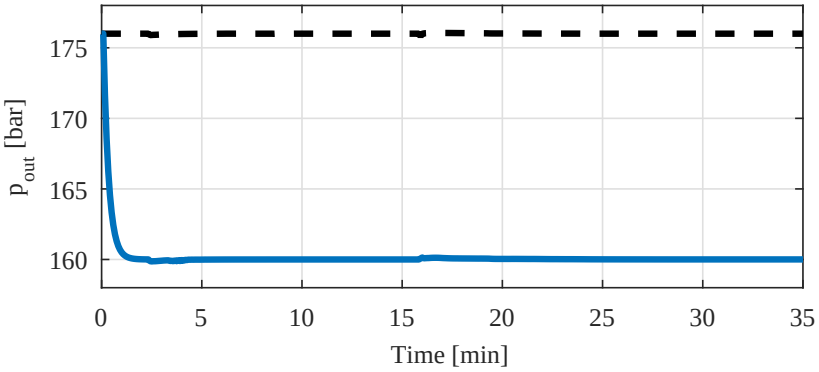

Figure 4.7: Results of the application of MPC1 - outlet header pressure. Dashed black line: regulatory control without MPC, solid blue line: regulatory control with MPC1

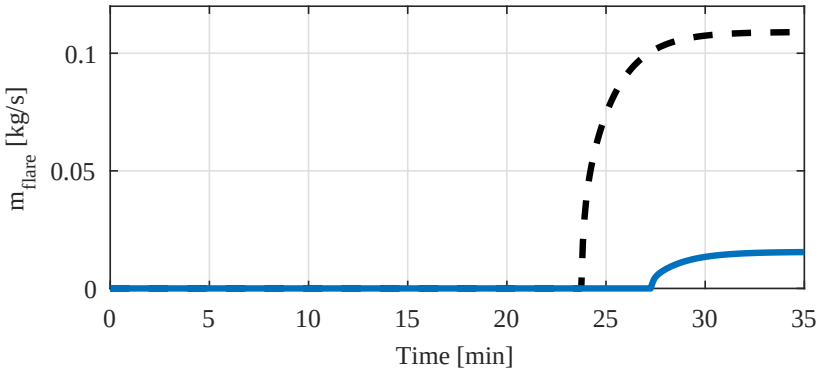

Figure 4.8: Results of the application of MPC1 - flared gas. Dashed black line: regulatory control without MPC, solid blue line: regulatory control with MPC1

4.1.2 MPC 2

This formulation is similar to the previous one in two points: the manipulated variables and constraints remain the same as in MPC1. But now energy consumption is minimized directly. To include the energy consumption, the objective function was changed. Since the energy E is a function of the consumed power P, the models relating $\mathbf{u}$ to P were included and a constraint that limits P was added. But, as explained in subsection 3.7.1, the static gain between P and the inlet pressure p_{in} changes signal depending on the operation point. Because of this nonlinearity the linearized model may induce the controller to take actions in the wrong direction. For that, the linearized model between P and p_{in} was disregarded. The targets for the manipulated variables were eliminated, except the one for the inlet pressure setpoint, to guarantee that p_{in} would return to its nominal value whenever possible.

Controlled and manipulated variables

The controlled variables y_{1-6} and the manipulated variables u_{1-8} remained the same.

Objective function

In this case, the objective J (equation 4.3) is to bring the control variables y to their references y_r (inside the band) and the ma-

nipulated variable u_1 to its target while minimizing the control variation $\Delta\mathbf{u}$ and the energy consumption E.

$$J = [\hat{\mathbf{y}} - \mathbf{y}_r]^T \mathbf{Q}_y [\hat{\mathbf{y}} - \mathbf{y}_r] + \Delta\mathbf{u}^T \mathbf{Q}_u \Delta\mathbf{u} + (u_1 - p_{in}^{nom})^T Q_t (u_1 - p_{in}^{nom}) + EQ_E \quad (4.3)$$

Control tuning

The weight for the minimization of the energy consumption was set to 1 and added as Q_E. The new diagonal matrices are:

$$\mathbf{Q}_y = diag([100, 100, 100, 100, 100, 100, 1])$$

$$\mathbf{Q}_u = diag([0.1, 0.001, 1, 1, 1, 1, 1, 1])$$

$$Q_t = 0.0005$$

$$Q_E = 1$$

In this formulation, $\hat{\mathbf{y}}$ are also kept in a band, as explained in section 2.1.4. So, if $0 \leq \hat{\mathbf{y}} \leq 0.93$ then $\mathbf{Q}_y = 0$.

Constraints

Since the energy consumption is a function of the power consumption, the lower and upper limits for power were added. As the power value is normalized, the lower limit is 0 and the upper limit is 1. All other constraints were maintained.

Results

The results obtained with the application of the second MPC formulation are shown in figures 4.9 to 4.14. In the figures, the dashed black lines represent the system's performance with the regulatory system only and the blue solid lines are the results of the application of the MPC2 formulation. In figures 4.3a, 4.4a, and 4.5a the doted black lines are the maximum limit of the surge indexes. These results are very similar to the ones obtained with the first MPC formulation, presented in subsection 4.1.1. Even though the power consumption was reduced, the controller could not keep the surge indexes below their upper limit.

This formulation was also tested with different tunings and in some cases the control actions were too aggressive while in others they were smooth but the system's response was too slow. Thus,

it was also difficult to tune manually the weights in MPC2. This suggests the use of a different method for this tuning, which is presented hereafter.

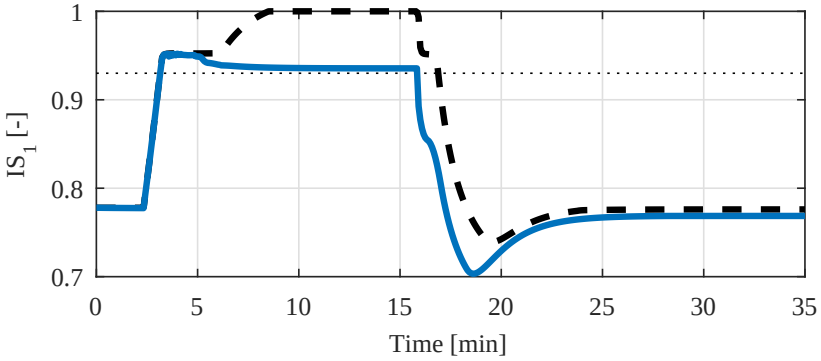

(a) Surge index

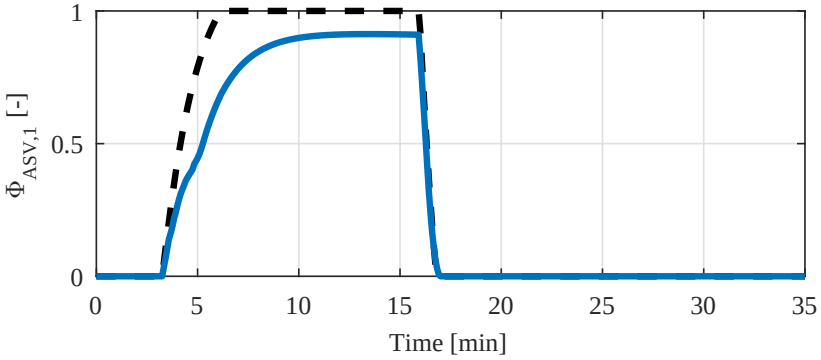

(b) Antisurge valve opening

Figure 4.9: Results of the application of MPC2 - Stage 1. Dashed black line: regulatory control without MPC, solid blue line: regulatory control with MPC2, doted black line: surge index upper limit

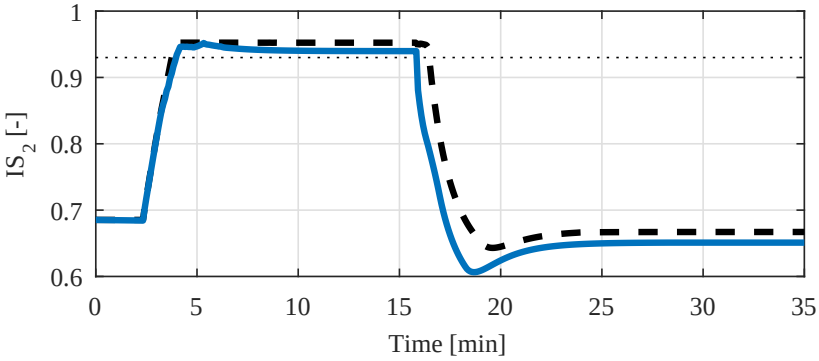

(a) Surge index

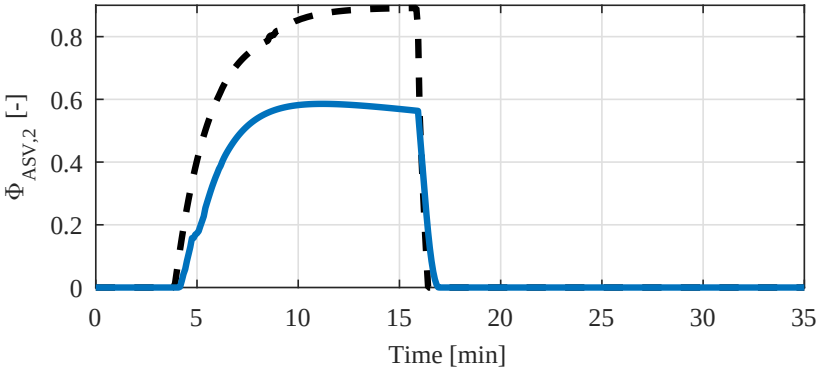

(b) Antisurge valve opening

Figure 4.10: Results of the application of MPC2 - Stage 2. Dashed black line: regulatory control without MPC, solid blue line: regulatory control with MPC2, doted black line: surge index upper limit

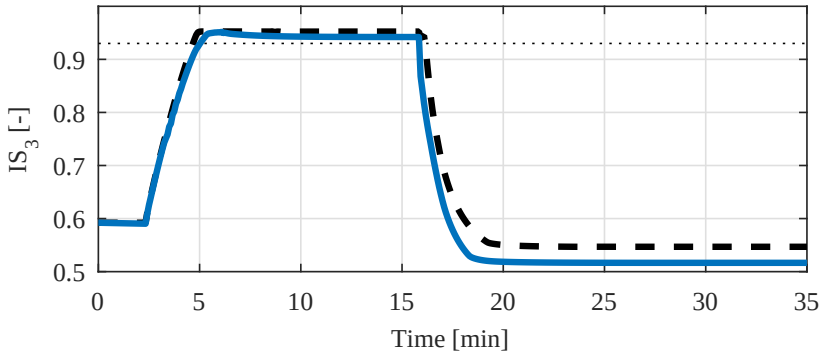

(a) Surge index

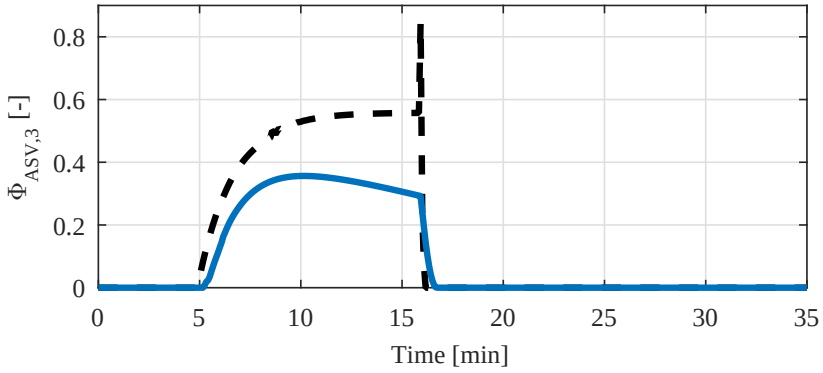

(b) Antisurge valve opening

Figure 4.11: Results of the application of MPC2 - Stage 3. Dashed black line: regulatory control without MPC, solid blue line: regulatory control with MPC2, doted black line: surge index upper limit

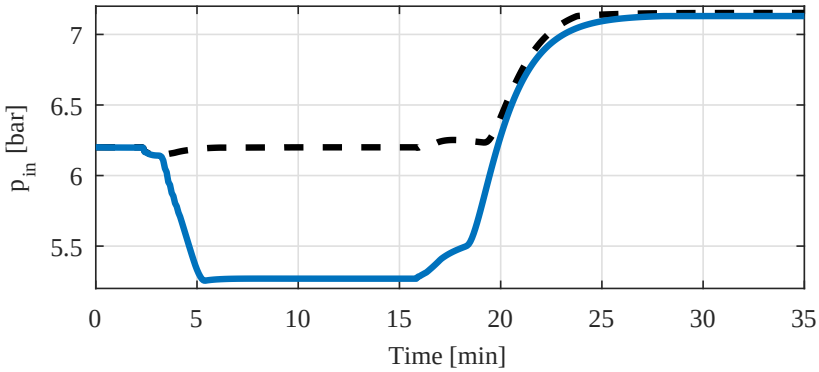

Figure 4.12: Results of the application of MPC2 - inlet header pressure. Dashed black line: regulatory control without MPC, solid blue line: regulatory control with MPC2

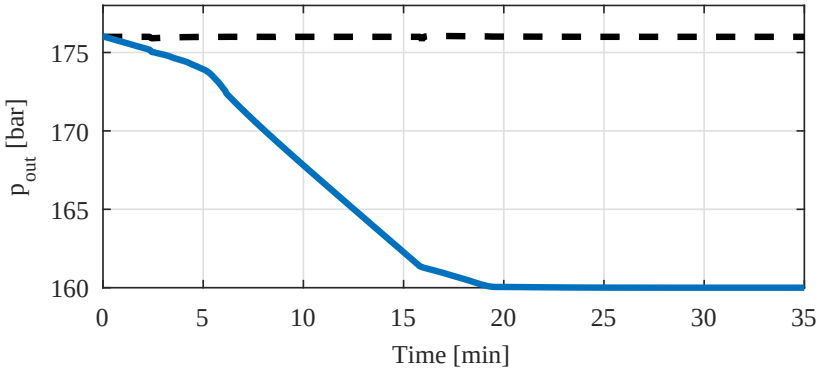

Figure 4.13: Results of the application of MPC2 - outlet header pressure. Dashed black line: regulatory control without MPC, solid blue line: regulatory control with MPC2

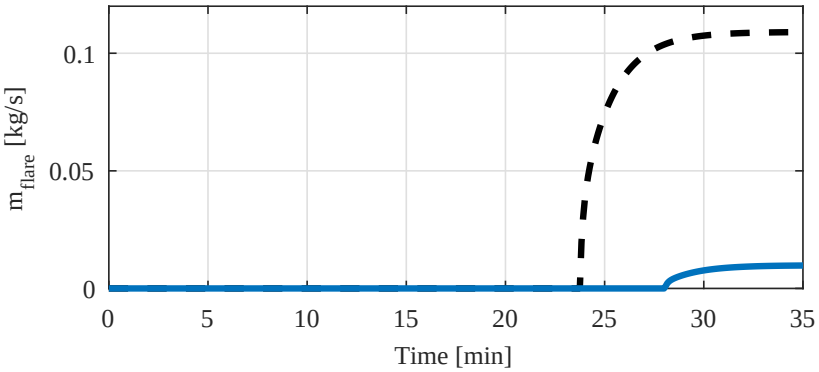

Figure 4.14: Results of the application of MPC2 - flared gas. Dashed black line: regulatory control without MPC, solid blue line: regulatory control with MPC2

4.1.3 MPC with satisficing tuning

The results shown in the previous subsections suggest that the MPC could be a good approach to improve the compression system control, however tuning the parameters of the weight matrices Q_y, Q_u, and Q_t have showed to be difficult, mainly because of the different dynamics and ranges that each variable has. To overcome this problem, the satisficing MPC tuning was used. The results of MPC1 were not improved with this technique, so only the results of MPC2 are shown in this section. The satisficing technique requires that acceptable ranges for each variable are defined, as explained in section 2.3. For this problem, the ranges were chosen as:

$$
\begin{aligned}
F_{sat}^{\Delta u} &= Nu[0.1^2 \;\; 20^2 \;\; 0.05^2 \;\; 0.05^2 \;\; 0.05^2 \;\; 0.05^2 \;\; 0.05^2 \;\; 0.05^2]^T \\
F_{sat}^{u_t} &= Nu[5^2]^T \\
F_{sat}^{y} &= N[0.01^2 \;\; 0.01^2 \;\; 0.01^2 \;\; 0.01^2 \;\; 0.01^2 \;\; 0.01^2]^T \\
F_{sat}^{E} &= N[0.5^2]^T
\end{aligned}
$$

where:

$F_{sat}^{\Delta u}$ - factor used to calculate the weights of Q_u for the control increments $\Delta\mathbf{u}$,

$F_{sat}^{u_t}$ - factor used to calculate the weight of Q_t for the target error $(u_1 - p_{in}^{nom})$,

F_{sat}^{y} - factor used to calculate the weights of Q_y for the reference error $[\hat{\mathbf{y}} - \mathbf{y}_r]$,

F_{sat}^{E} - factor used to calculate the weight of Q_E for energy consumption minimization E,

Nu - control horizon,

N - prediction horizon.

Results

The results obtained by tuning MPC2 with the satisficing tuning technique are shown in figures 4.15 to 4.21. The performance of MPC1 was not improved by the technique so only the results obtained with MPC 2 are shown. The black dashed lines correspond to the compression system with the regulatory control only. The blue dash-dot lines correspond to the results of the application of MPC2 with manual tuning while the red solid lines are the results of the application of MPC2 with satisficing tuning.

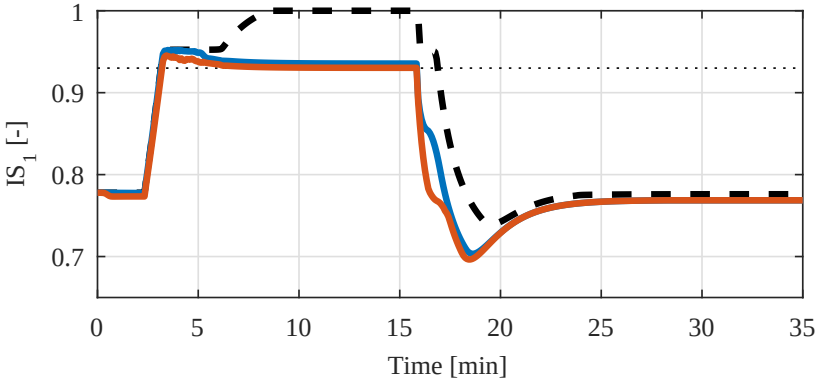

(a) Surge index

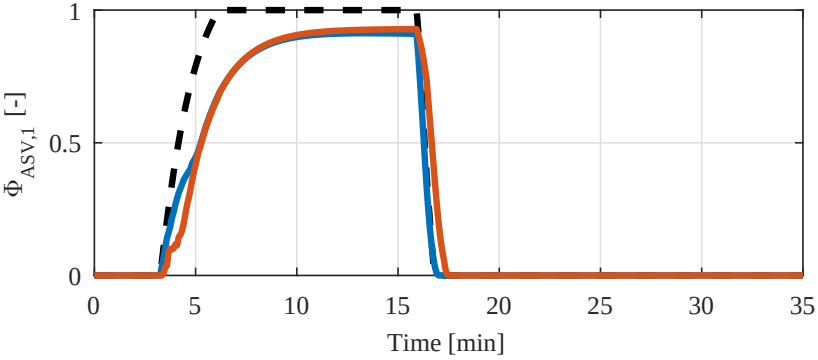

(b) Antisurge valve opening

Figure 4.15: Results of the satisficing tuning applied on MPC2 - Stage 1. Dashed black line: regulatory control without MPC, solid blue line: regulatory control with MPC2 tuned manually, solid red line: regulatory control with MPC2 tuned with the satisficing technique, doted black line: surge index upper limit

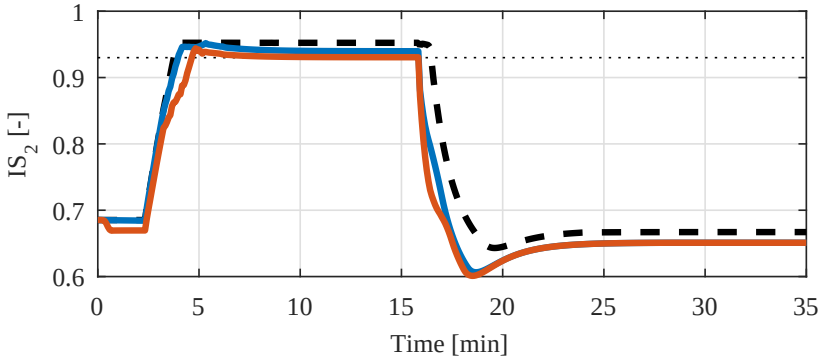

(a) Surge index

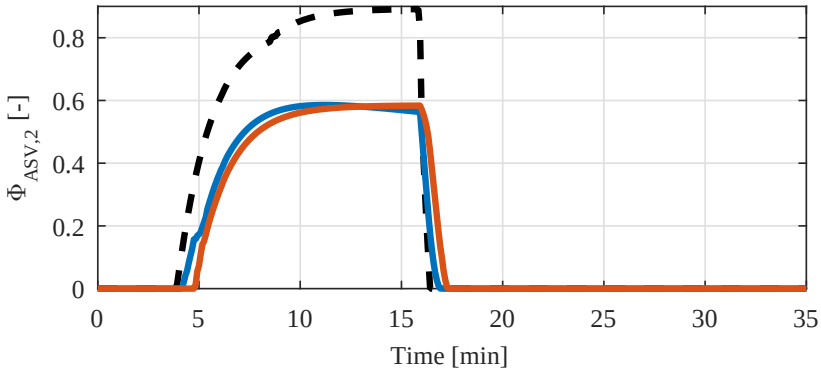

(b) Antisurge valve opening

Figure 4.16: Results of the satisficing tuning applied on MPC2 - Stage 2. Dashed black line: regulatory control without MPC, solid blue line: regulatory control with MPC2 tuned manually, solid red line: regulatory control with MPC2 tuned with the satisficing technique, doted black line: surge index upper limit

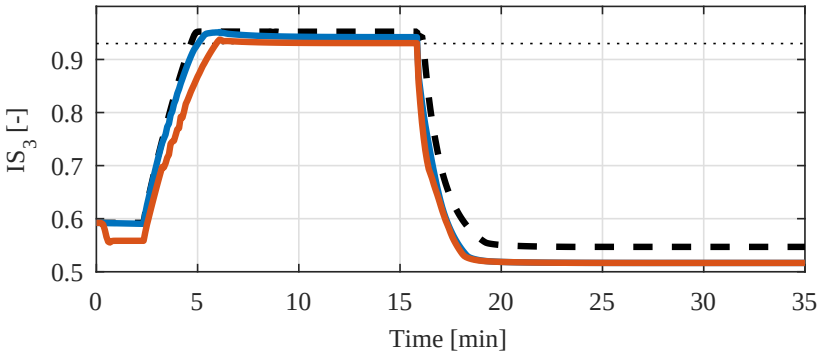

(a) Surge index

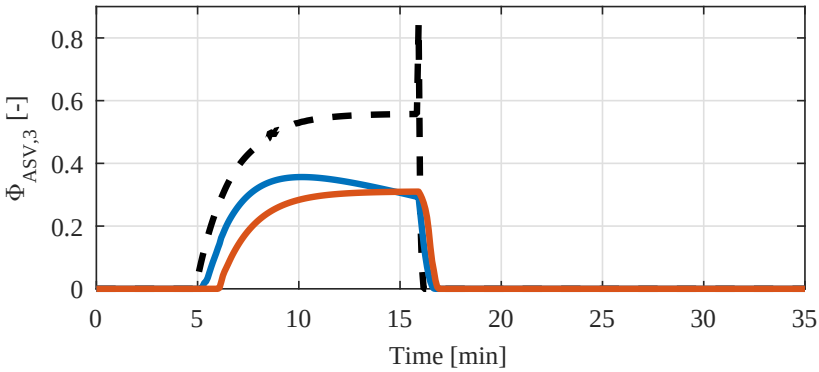

(b) Antisurge valve opening

Figure 4.17: Results of the satisficing tuning applied on MPC2 - Stage 3. Dashed black line: regulatory control without MPC, solid blue line: regulatory control with MPC2 tuned manually, solid red line: regulatory control with MPC2 tuned with the satisficing technique, doted black line: surge index upper limit

The performance of the controller was improved by the satisficing tuning. The overshoot of the surge indexes was reduced, and the MPC2 was able to maintain the indexes at their limit in steady state.

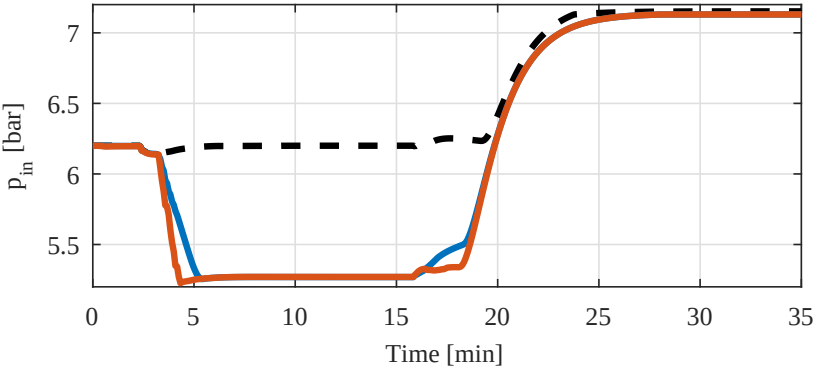

Figure 4.18: Results of the satisficing tuning applied on MPC2 - inlet header pressure. Dashed black line: regulatory control without MPC, solid blue line: regulatory control with MPC2 tuned manually, solid red line: regulatory control with MPC2 tuned with the satisficing technique

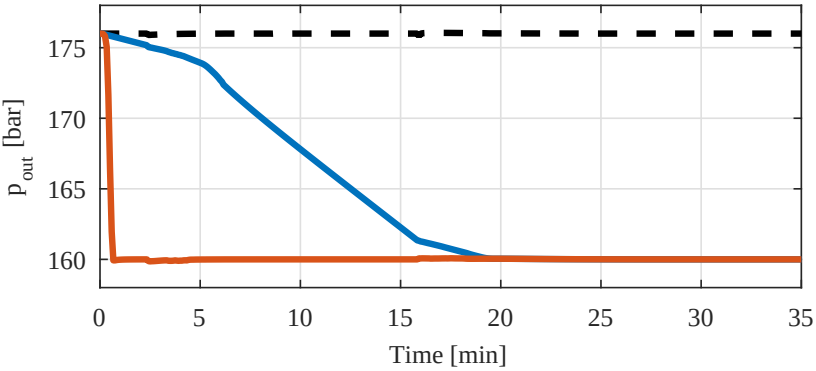

Figure 4.19: Results of the satisficing tuning applied on MPC2 - outlet header pressure. Dashed black line: regulatory control without MPC, solid blue line: regulatory control with MPC2 tuned manually, solid red line: regulatory control with MPC2 tuned with the satisficing technique

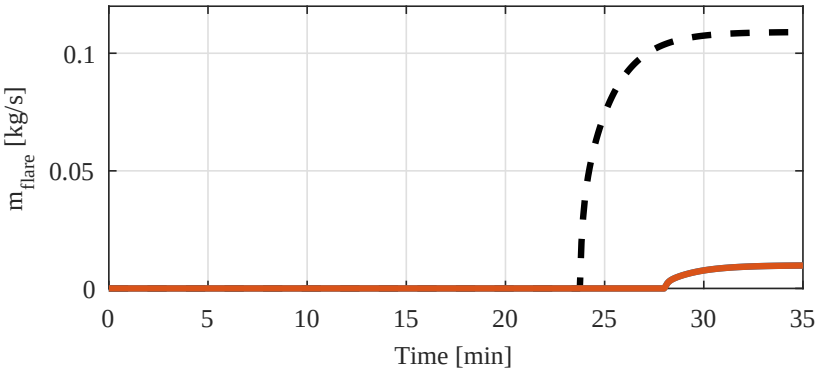

Figure 4.20: Results of the satisficing tuning applied on MPC2 - flared gas. Dashed black line: regulatory control without MPC, solid blue line: regulatory control with MPC2 tuned manually, solid red line: regulatory control with MPC2 tuned with the satisficing technique

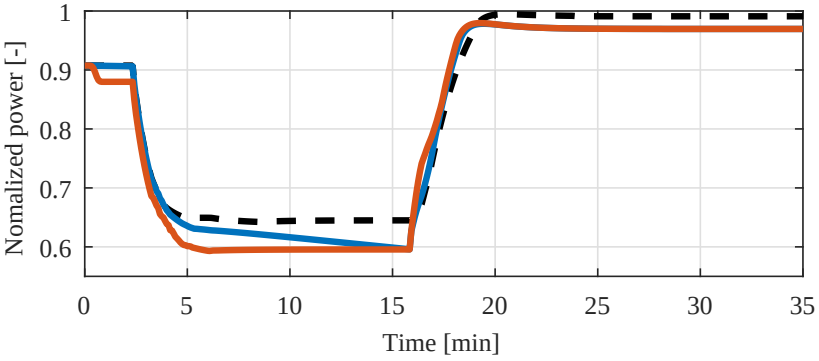

Figure 4.21: Results of the satisficing tuning applied on MPC2 - consumed power. Dashed black line: regulatory control without MPC, solid blue line: regulatory control with MPC2 tuned manually, solid red line: regulatory control with MPC2 tuned with the satisficing technique

Figure 4.21 shows the power consumed by the compression system and, even though MPC2 minimizes it directly, there is no significant difference in the consumption. Due to the changes executed in p_{in}, both MPC controllers were able to decrease the amount of

Table 4.1: MPC performance comparison

	Regulatory	MPC1	MPC2 manual	MPC2 satisficing
Energy consumption	100%	96.24%	97.92%	97.01%
Flared gas	100%	9.22%	5.15%	5.15%
Recycled gas	100%	60.07%	66.23%	63.46%

flared gas.

Table 4.1 summarizes the performance of the proposed MPCs. The results obtained by simulating the system without any MPC controller were considered the worst case scenario, therefore they represent 100% of energy consumption, gas flaring, and gas recycling. For example, the application of the MPC2 algorithm cause the system to recycle only 63.46% of the total amount of gas recycled by the system with the regulatory control only. The application of MPC1 resulted in a smaller energy consumption than the application of MPC2 because MPC1 recycled less gas. However, MPC1 fail to keep the surge indexes below their maximum limit, as shown in figures 4.3a to 4.5a. MPC2 spends more energy recycling more gas to keep $IS \leq 0.93$, as shown in figures 4.15a to 4.17a. The performance comparison presented in table 4.1 shows little difference between MPC2 manual and MPC2 satisficing. The main advantage of the satisficing tuning technique is that it provided a satisfactory tune for the MPC controller faster then other heuristic techniques.

4.2 ROBUSTNESS ANALYSIS

To further investigate the proposed solutions a robustness analysis was made. To do so, errors in critical parameters were introduced. These parameters were selected based on the practical knowledge of the process engineers regarding the studied compression system:

- Molecular weight of the gas - $\pm 15\%$
- Moment of inertia of the compressors turbines - $\pm 40\%$
- Antisurge valves coefficients - $\pm 20\%$
- Scrubber volumes - $\pm 40\%$

The linearized prediction model was obtained at the same equilibrium point used by the manufacturer to obtain the compressor's data sheet, that is the same gas molecular weight, flow rate, and pressure to be the nominal values defined by the manufacturer. The scenario presented in the previous section was simulated 50 times. Each time, randomly chosen errors were added to the listed parameters. In each simulation the prediction model remained the same but the plant was different. The error added to each parameter was randomly chosen in a rectangular distribution between the defined limits. Figures 4.22a to 4.28 show the results of the robustness test applied to MPC2. The black solid lines represent the regulatory control results and the colored dashed lines are the results of the MPC2 in several simulations. Even though there are differences in the results, they are very similar. The optimization problem created to obtain the control increments was never infeasible and MPC controller worked properly at every simulation.

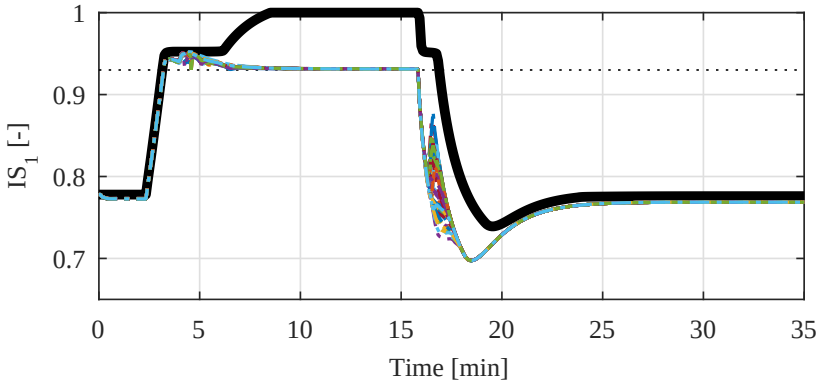

(a) Surge index

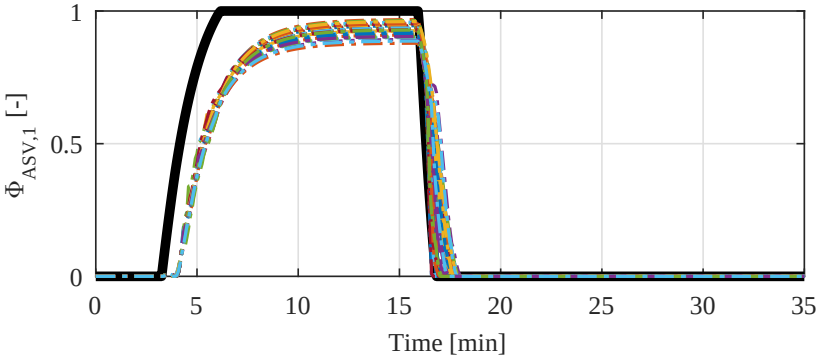

(b) Antisurge valve opening

Figure 4.22: Results of the robustness test - stage 1. Solid black line: regulatory control without MPC, colored dashed lines: regulatory control with MPC2, doted black line: surge index upper limit

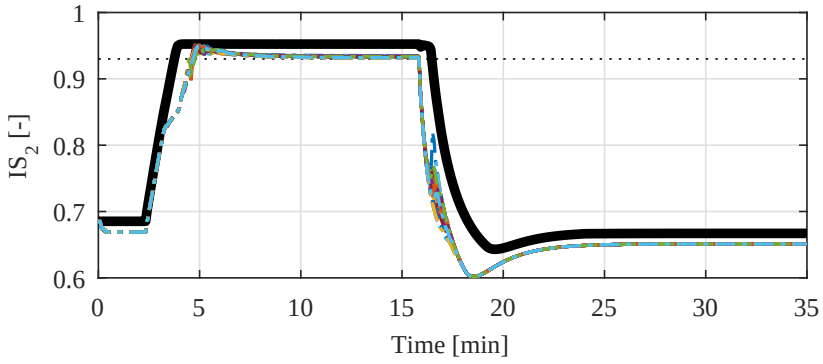

(a) Surge index

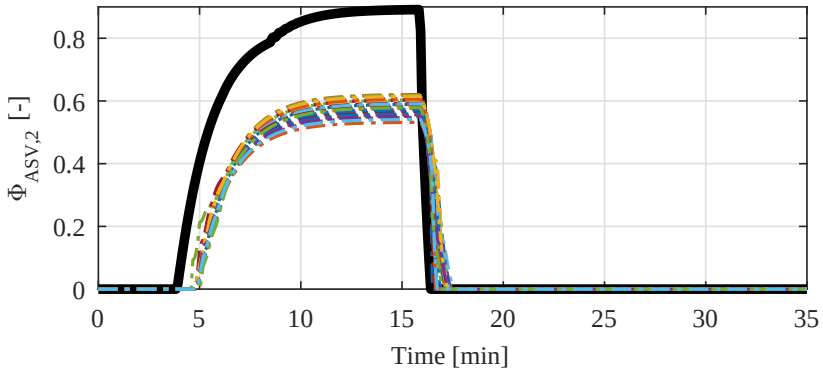

(b) Antisurge valve opening

Figure 4.23: Results of the robustness test - stage 2. Solid black line: regulatory control without MPC, colored dashed lines: regulatory control with MPC2, doted black line: surge index upper limit

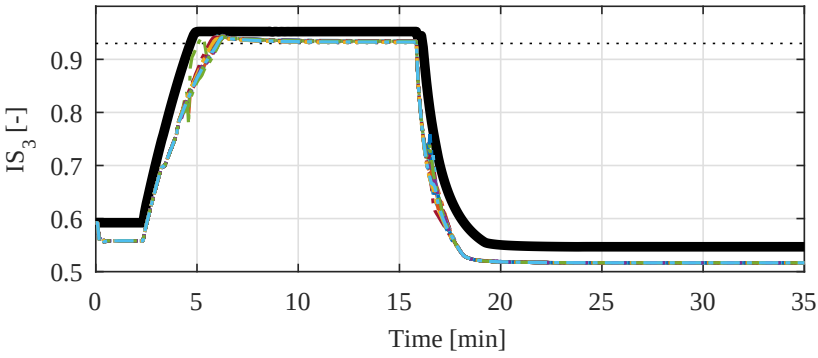

(a) Surge index

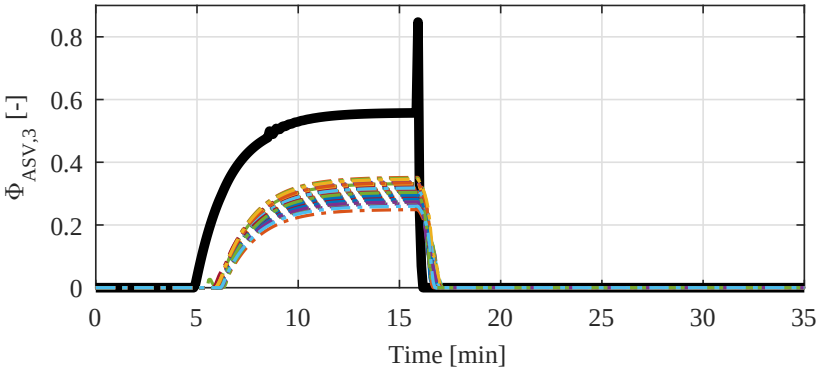

(b) Antisurge valve opening

Figure 4.24: Results of the robustness test - stage 3. Solid black line: regulatory control without MPC, colored dashed lines: regulatory control with MPC2, doted black line: surge index upper limit

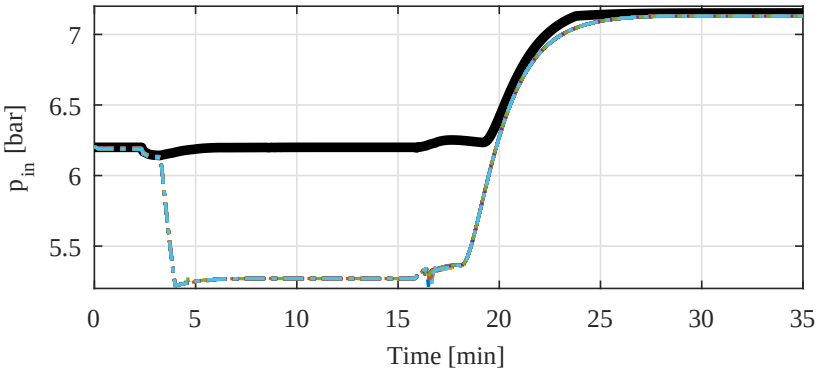

Figure 4.25: Results of the robustness test - inlet header pressure. Solid black line: regulatory control without MPC, colored dashed lines: regulatory control with MPC2

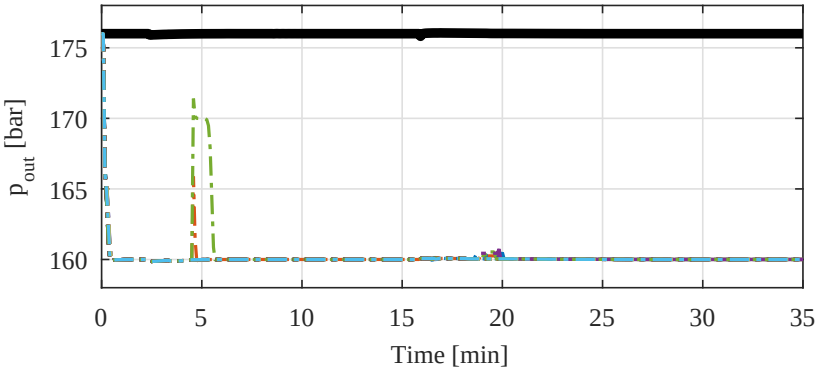

Figure 4.26: Results of the robustness test - outlet header pressure. Solid black line: regulatory control without MPC, colored dashed lines: regulatory control with MPC2

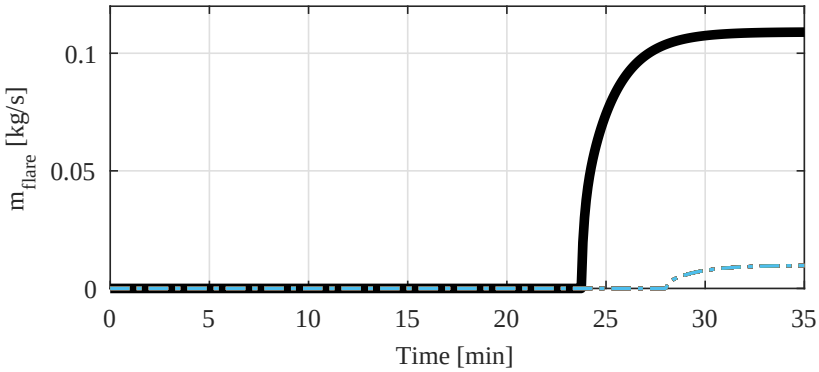

Figure 4.27: Results of the robustness test - flared gas. Solid black line: regulatory control without MPC, colored dashed lines: regulatory control with MPC2

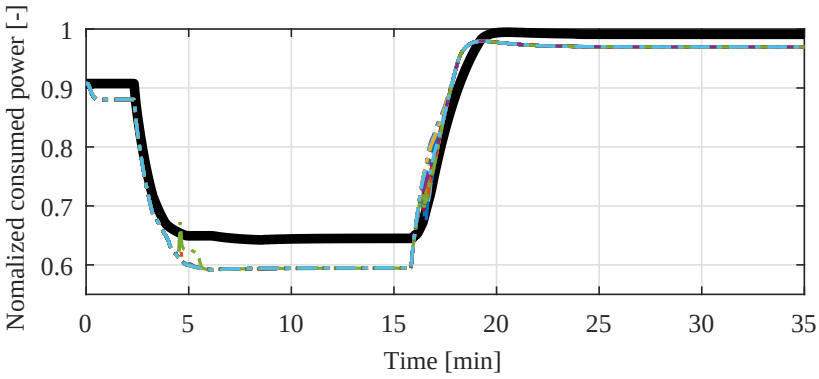

Figure 4.28: Results of the robustness test - consumed power. Solid black line: regulatory control without MPC, colored dashed lines: regulatory control with MPC2

With these results it is expected that the MPC2 could be applied to the real compression system. The same test was performed with the MPC1, but in this case the results showed that this solution is less robust. The optimization problem was infeasible in the majority of the simulations and the MPC algorithm could not calculate the control actions for control the system.

4.3 FINAL COMMENTS

This chapter presented the implementations of two MPC controllers and the results of their application. It also presented the results of the applications of the satisficing tuning technique and the results of a robustness test.

In the first MPC formulation, the total energy is minimized indirectly as the controller drives the manipulated variables to values that minimize the power consumption. This formulation was tried so that the nonlinearities between the power consumption and the inlet header pressure would not affect the system's performance, since the model that relates them would not be used. But these results were not satisfactory and could not be improved by the satisficing tuning. MPC1 also failed the robustness test.

The second MPC formulation had better results than the first one. In MPC2 formulation the energy consumption was included in the objective function so it could be minimized directly. MPC2's performance was improved by the application of the satisficing technique. MPC2 passed the robustness test because it worked well even when critical parameters of the model were changed.

5 CONCLUSIONS

In this dissertation a MPC controller was proposed to improve the performance of an compression system. For that, a detailed description of the system's mathematical model was presented, along with the analysis of the system's behavior and of the potential controlled and manipulated variables to be used by the MPC controllers to achieve the control objectives. A tuning technique was also tested to improve the system's performance and a robustness test was performed. Two MPC formulations were presented. In the first one, the energy consumption is minimized indirectly while in the second formulation the energy consumption is minimized directly in the objective function. Only the second formulation achieved the control objectives and proved to be robust to the disturbance applied.

The main contributions of this dissertation are:

- the modeling and analysis of a complete compression system from a real oil production platform,
- the formulation of a MPC controller as a control layer above the regulatory system, running at a higher sampling period,
- the application of a tuning technique that improved the system's performance.

In the literature, several compressor models can be found, but they usually describe the compression on a single stage. In this dissertation, the modeled system consists of two parallel 3-stage compressors with an inlet header and an outlet header. Chapter 3 presented the modeling and analysis of the compression system. This modeling resulted in two publications [25, 35].

This work also presented a MPC controller capable of preventing surge and while minimizing energy consumption. Chapter 2 presented important concepts used in the MPC formulation along with the satisficing technique to tune the MPC controller. The application of this technique improved the MPC controller's performance. The possibility of implementing the MPC as a control layer above the regulatory PID controllers with a greater sampling time was investigated. Even though the surge phenomena occurs in less than a second and the MPC was set to run every 5 seconds, the MPC's predictive ability allowed the controller to drive the system to a safer operation point, preventing surge.

Regarding practical outcome, because of the success of the proposed control strategy in the simulated plant, the algorithm will

be implemented in a real-time control software. After exhaustive testings, it may be applied on a real oil and gas production platform. Regarding academic follow-up, it will be performed a test to assess the MPC controller's performance in a scenario of a compression train shutdown.

REFERENCES

1 AGUIAR, M. A.; CODAS, A.; CAMPONOGARA, E. Systemwide optimal control of offshore oil production networks with time dependent constraints. *IFAC-PapersOnLine*, v. 48, n. 6, p. 200 – 207, 2015.

2 GRAVDAHL, J. T. *Modeling and Control of Surge and Rotating Stall in Compressors*. Thesis (PhD) — NTNU-Norwegian University of Science and Technology, Trondheim, Norway, 1998.

3 RAMUSSEN, P. C.; KURZ, R. Centrifugal compressor applications - ustream and midstream. *38th Turbomachinery Symposium*, 2009.

4 GRAVDAHL, J. T. et al. Modeling for surge control of centrifugal compressors:comparison with experiment. *Proceedings of the 39th IEEE Conference on Decision and Control*, 2000.

5 BUDINIS, S.; THORNHILL, N. F. Control of centrifugal compressors via model predictive control for enhanced oil recovery applications. *Proceeding of the 2nd IFAC Workshop on Automatic Control in Offshore Oil and Gas Production*, Florianopolis, SC, Brasil, 2015.

6 TORRISI, G. et al. Model predictive control approaches for centrifugal compression systems. *Proceedings of the 54th IEEE Conference on Decision and Control*, 2015.

7 GREITZER, E. M. Surge and rotating stall in axial flow compressors—part i: Theoretical compression system model. *Journal of Engineering for Power - Transactions of the ASME*, p. 190–198, 1976.

8 GRAVDAHL, J. T.; EGELAND, O. Speed and surge control for a low order centrifugal compressor model. *Model Identification and Control, vol.19, n1, 13-29*, 1998.

9 BOINOV, K. O. et al. Surge control of the electrically driven centrifugal compressor. *IEEE TRANSACTIONS ON INDUSTRY APPLICATIONS, VOL. 42, NO. 6, NOVEMBER/DECEMBER 2006*, 2006.

10 DORMIDO, S. Una revisión de las tecnologías de control predictivo basado en modelos en la industria. *Wokshop sobre estado y perspectivas del control predictivo*, Valladolid, Spain, 1987.

11 OVERVAG, T. F. *Centrifugal Compressor Load Sharing with the use of MPC*. Thesis (PhD) — NTNU-Norwegian University of Science and Technology, Trondheim, Norway, 2013.

12 CORTINOVIS, A. et al. Model predictive anti-surge control of centrifugal compressors with variable-speed drives. *Proceedings of the 2012 IFAC Workshop on Automatic Control in Offshore Oil and Gas Production*, Trondheim, Norway, 2012.

13 SMEULERS, J.; BOUMAN, I. W.; ESSEN, H. van. Model predictive control of compressor installations. *Proceedings of the IMeche 1999*, Trondheim, Norway, 1999.

14 SANTOS, J. E. W. dos. *Método de Ajuste para MPC baseado Em Multi-Cenários para Sistemas Não Quadrados*. Dissertation (Master) — Universidade Federal do Rio Grande do Sul, Porto Alegre, 2016.

15 GARRIGA, J. L.; SOROUSH, M. Model predictive control tuning methods: A review. *Industrial and Engineering Chemistry Research*, n. 49, p. 3505–3515, 2010.

16 LIMA, M. L. et al. Distributed Satisficing MPC. *IEEE Transactions on Control Systems Technology*, v. 23, n. 1, p. 305–312, 2015.

17 BERGH, L. G.; MACGREGOR, J. F. Constrained minimum variance controllers: Internal model structure and robustness properties. *Ind. Eng. Chem. Res.*, v. 26, p. 1558–1564, 1987.

18 PALMOR, Z. Properties of optimal stochastic control systems with dead-time. *Automatica*, v. 18, p. 107–116, 1982.

19 CAMACHO, E.; BORDONS, C. *Model Predictive Control*. Berlin: Springer, 2007.

20 FLESCH, R. C. C. *Contribuicoes ao Controle de Sistemas Monovariaveis e Multivariaveis com Atraso de Transporte*. Thesis (PhD) — Universidade Federal de Santa Catarina, 2012.

21 LIMA, D. M. et al. Improving Robustness and Disturbance Rejection Performance with Industrial MPC. *Congresso Brasileiro de Automática*, 2014.

22 MORARI, M.; LEE, J. H.; GARCIA, C. E. *Model Predictive Control*. New Jersey: Prentice Hall, 2002.

23 M.P.BOYCE et al. Practical aspects of centrifugal compressors surge and surge control. *Proceedings of the Twelfth Turbomachinery Symposium*, 1983.

24 HANSEN, C. *Dynamic Simulation of Compressor Control Systems*. Thesis (PhD) — Aalborg University Esbjerg, Niels Bohrs vej 86700 Esbjerg, Denmark, 2008.

25 PLUCENIO, A. et al. Modeling and control of a gas compression station used in an oil platform. *Congresso Brasileiro de Automática*, Vitoria, ES, Brasil, 2016.

26 HAFAIFA, B. R. A.; MOULOUD, G. Modeling of surge phenomena in a centrifugal compressor: experimental analysis for control. *Systems Science and Control Engineering,* $2:1,632-641$, 2014.

27 GRAVDAHL, J. T. et al. Modeling for surge control in free-spool centrifugal compresssors:experimental validation. *JOURNAL OF PROPULSION AND POWER*, 2004.

28 JIANG, J. K. W.; DOUGAL, R. A. Dynamic centrifugal compressor model for system simulation. *Journal of Power Sources*, 2005.

29 PAPARELLA, F. et al. Load sharing optimization of parallel compressors. *European Control Conference, ECC*, 2013.

30 NIEUWENHUIZEN, M. *Parameter analysis and identification of the Greitzer model by analogy with the Van der Pol equation*. Thesis (PhD) — Technische Universiteit Eindhoven, Department Mechanical Engineering, Dynamics and Control Technology Group, De Rondom 70, 5612 AP Eindhoven, Netherlands, 2008.

31 BOHAGEN, B. *Active surge control of centrifugal compression systems*. Thesis (PhD) — NTNU-Norwegian University of Science and Technology, Trondheim, Norway, 2007.

32 DRESSER. *Control Valve Sizing Handbook*. Huston: Dresser Masoneilan, 2009.

33 PLUCENIO, A. *Desenvolvimento de Tecnicas de Controle Nao Linear para Elevacao de Fluidos Multifasicos*. Thesis (PhD) — Programa de Pos-Graduacao em Engenharia de Automacao e Sistemas, DAS, Universidade Federal de Santa Catarina, Florianopolis-SC-Brasil, 2010.

34 YANG, B. P.; PLUCENIO, A. Practical non-linear model predictive control pnmpc: Algorithm implementations. *Congresso Brasileiro de Automática*, Vitoria, ES, Brasil, 2016.

35 PLUCENIO, A. et al. Advanced control applied to a gas compression station of a production platform. *Congresso Brasileiro de Automática*, Vitoria, ES, Brasil, 2016.